

Damage localisation using elastic waves propagation method. Experimental techniques.

Wieslaw Ostachowicz ^{*‡} Pawel Malinowski [‡] and Tomasz Wandowski [‡]

^{*} Faculty of Navigation, Gdynia Maritime University, Gdynia, Poland

[‡] Department of Mechanics of Intelligent Structures, Polish Academy of Sciences, Gdansk, Poland

Abstract In this chapter methods of Structural Health Monitoring using elastic wave propagation method are presented. Different techniques are presented that are used for elastic wave generation and sensing. In the case of elastic waves sensing presented methods are divided into contact and non contact (optical). Wide description of measuring methods that are based on laser vibrometry can be also find. This chapter also includes description of damage localisation algorithms. Also phenomenon of elastic wave propagation in the structural elements is widely described. In this chapter different types of elastic wave propagating in structural elements are presented however attention is focused on Lamb waves. Chapter includes lots of experimental results related to measurements and visualisation of elastic waves propagation as well as results of damage localisation.

1 Structural Health Monitoring based on elastic waves propagation

Structural Health Monitoring (SHM) is technique that allow to conduct continuous monitoring of engineering structures. The monitoring process is realized in real time during the normal usage of structures. Structural Health Monitoring systems are very often compared with human nervous system in which nerves provide information about pain. These information are next processed in the human brain. In SHM systems network of transducers can be compared with human nerves and signal processing unit with the human brain. SHM systems very often utilize elastic wave propagation method in order to assess the state of the whole structure or its single elements. Elastic wave propagation method is based on fact that any kind of

discontinuities in elements of structure cause changes in elastic wave propagation. These changes in the form of reflections or amplitude decrease can be sensed and used in damage detection or localisation algorithms. This method is very sensitive therefore damage in early stage of growth before it endangers the safety of structures can be detected. For comparison vibration based SHM systems are less sensitive to damage. Therefore elastic wave propagation method is so promising technique.

Elastic waves are very often excite and sensed using piezoelectric transducers that are thin, light and can be simply mounted on or embedded in the structural elements. Except piezoelectric transducers also other techniques are used but descriptions of these method are included in the next section. SHM system based on elastic wave propagation phenomenon can be divided into two types: passive and active. In the passive systems network of transducers (sensors) only listen the structure and sensing signals representing elastic waves that propagate in the structure (Gangadharan et al., 2009), (Ding et al., 2004). Passive systems for example are utilized for impact localisation. Examples of impact in aircraft structures are: bird strike or spanner dropped by the mechanic. In active systems diagnostic signals are excited and sensed using transducers network and such systems are used for assessment of structural health (Kirikera et al., 2006). In SHM five levels of diagnose can be distinguished (Rytter, 1993), (Worden and Dulieu-Barton, 2004):

- detection,
- localisation,
- identification,
- damage size extraction,
- prediction of remaining structure lifetime.

Many researchers all around the world are interested in application of phenomenon of elastic wave propagation to assess the state of real structures without the needs of exclude the structure from its normal exploitation. However numerous difficulties with real structures cause that research is very often connected only with parts of the structure or with simple real structures. Complexity of real structures cause lot of problems with damage localisation using elastic waves. Complex geometry of structure, stiffeners, bolts, rivets and welds are sources of wave reflections and amplitude decreases. Many problems are related to sensor integration with structure,

reliability of sensors in spite of mechanical loads influence, material fatigue, corrosive environment, wide range of exploitation temperatures. In the case of aerial structures very important is also problem of very restrictive airworthiness directives that limit the possibilities of installation of SHM systems. However in the case of structural elements some algorithms for damage detection, localisation and identification of type or size of damage were developed with success. Problem of damage detection and localisation in beams was solved by (Giurgiutiu, 2008), (Lestari and Qiao, 2005), (Palacz et al., 2005), (Su et al., 2007). Damage localisation algorithms were also developed for the structures in the form of pipes or pipelines (Cau et al., 2006), (Qing et al., 2009), (Siqueira et al., 2004), (Thien, 2006). Elastic waves are also utilized in order to detect and localise damage in rails (Lee et al., 2009), (Zumpano and Meo, 2006). Moreover elastic waves are utilized for damage localisation in metallic plates and plates made out of composite materials: (Giurgiutiu, 2008), (Giurgiutiu et al., 2007), (Ihn and Chang, 2008), (Ihn and Chang, 2004), (Ostachowicz et al., 2009), (Ostachowicz and Kudela, 2007), (Salas and Cesnik, 2009), (Yu et al., 2008).

2 Elastic waves

As was mentioned in previous section elastic waves are very often utilized in SHM systems. Elastic waves propagating in the structure carry important information about damage presence, its localization, size or type. Therefore it is so important to understand the types of elastic waves that can propagate in the structural elements. Different types of elastic waves can be characterized by different sensitivity on the specific types or location of damage.

In unlimited three dimensional solids two types of wave can propagate: longitudinal waves and shear waves. The classification is connected with direction of particles vibration in relation to direction of elastic wave propagation. In the case of longitudinal waves particle displacement direction is compatible with direction of propagation see Figure 1a). For the shear waves direction of particles displacement is perpendicular to direction of waves propagation as it is shown in the Figure 1b).

Situation is more complicated if one surface of three dimensional solid is limited. In such a case due to internal reflection of elastic waves raise up elastic waves with complex displacement field. Two types of elastic waves can be distinguished: Rayleigh waves and Love waves. Rayleigh waves are the type of elastic waves that propagate on the surface of solids which thickness is many times larger than length of propagating waves. Vibrating particles due to wave motion move along the trajectories in the form of circles Figure

1c). Characteristic feature of Rayleigh waves is effect of amplitude decay with the growing depth. Largest values of Rayleigh waves amplitudes are observed on the surface. Love waves have more complex displacement field than in the case of Rayleigh waves. Displacement field of Rayleigh waves can be presented in 2D however for illustration of displacement related to Love waves three dimensional plot is needed (Figure 1d). In the case of Love waves similarly like for Rayleigh waves amplitude decay with the growing depth of structure.

In the case of 3D solid limited by two surfaces (e.g. plates, shells) situation changes radically. In such structures longitudinal waves and shear waves propagate simultaneously. But in this case shear waves can be divided into shear horizontal waves (SH) and shear vertical waves (SV). For both types of waves direction of particles vibration is perpendicular to direction of elastic wave propagation. In the case of SH waves particles of structure vibrate in horizontal direction and in the case of SV wave particles vibrate in vertical direction. As result of internal reflections of longitudinal waves and shear vertical waves new forms of waves are created - Lamb waves. Its name is connected with the Horacy Lamb that discovered these waves and formulated theory of its propagation in year 1917. These waves exist as symmetrical (Figure 1e)) and antisymmetrical modes (Figure 1f)). Number of this modes is infinite but number of propagating modes depends on product of excitation frequency and thickness of limited structure. Both symmetrical and antisymmetrical modes of Lamb waves are dispersive what means that its velocity of propagation changes with frequency. Dispersive character of both modes can be described by so called Rayleigh-Lamb equations 1, 2:

$$\frac{\tan(qd)}{q} + \frac{4k^2 p \tan(pd)}{(q^2 - k^2)^2} = 0 \quad (1)$$

$$q \tan(qd) + \frac{(q^2 - k^2)^2 \tan(pd)}{4k^2 p} = 0 \quad (2)$$

where: d - half of plate thickness [m], k - wave number [$1/m$].

Wave number can be calculated using formula:

$$k = \frac{\omega}{c_p} \quad (3)$$

Coefficients: p and q can be calculated using following formulas: 4 and 5.

$$p^2 = \left(\frac{\omega}{c_L}\right)^2 - k^2 \quad (4)$$

$$q^2 = \left(\frac{\omega}{c_T}\right)^2 - k^2. \quad (5)$$

where: c_L and c_T propagation velocities of longitudinal and shear wave respectively calculated based on: 6 i 7.

$$c_L = \sqrt{\frac{\lambda + 2\mu}{\rho}}. \quad (6)$$

$$c_T = \sqrt{\frac{\mu}{\rho}}. \quad (7)$$

where: ρ - density [kg/m^3], λ and μ Lamé constants calculated from equations:

$$\lambda = \frac{\nu E}{(1 + \nu)(1 - 2\nu)}, \quad (8)$$

$$\mu = \frac{E}{2(1 + \nu)}, \quad (9)$$

where: E - Young modulus [N/m^2], ν - Poisson ratio [-].

Solution of Rayleigh-Lamb equations 1 and 2 allow to plot dispersion curves. These curves illustrate the changes of group and phase velocity Lamb wave modes in relation to plate thickness and excitation frequency. Computer code solving Rayleigh-Lamb equation has been developed in MATLAB environment and has been based on algorithm presented in (Rose, 2004).

Dispersion curves were calculated for aluminium alloy EN AW-5754 with following material properties: Poisson ratio $\nu = 0.33$, density $\rho = 2680 \text{ kg/m}^3$, Young modulus $E = 70500 \text{ N/m}^2$, thickness $d = 0.001 \text{ m}$. For these parameters velocities of longitudinal and shear waves were calculated: $C_L = 6420 \text{ m/s}$ i $C_T = 3040 \text{ m/s}$. Dispersion curves for group and phase velocities were presented respectively in Figure 2 and Figure 3. After analysis it can be noticed that up to frequency 15 MHz in 1 mm thick plate six symmetrical (S_0 - S_5) and anti-symmetrical (A_0 - A_5) modes propagate. Up to almost 2 MHz in the 1 mm thick plate only two fundamental modes symmetrical and antisymmetrical denoted as S_0 and A_0 propagate. For the higher frequencies higher modes propagate in the plate.

When phase velocities of propagating Lamb wave modes are known in simple way displacement distributions through the thickness for chosen mode and frequency can be calculated. Displacement distributions can be

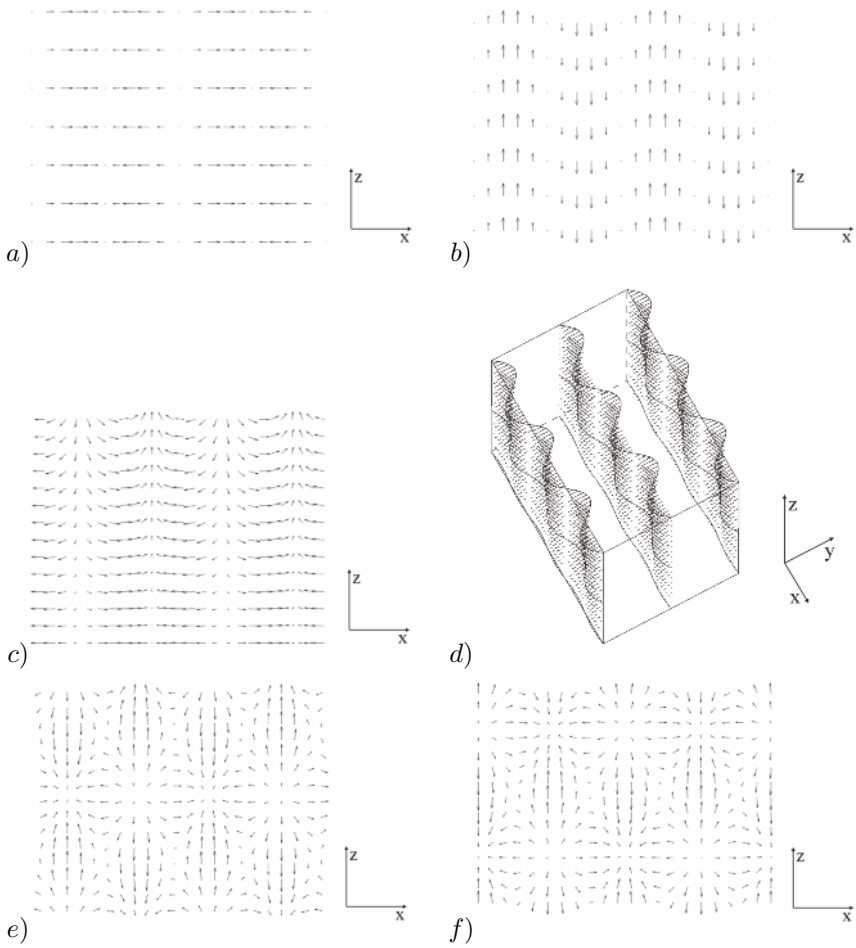


Figure 1. Displacement fields for: a) longitudinal waves, b) shear waves, c) Rayleigh waves, d) Love waves, e) symmetric Lamb waves mode, f) anti-symmetric Lamb waves mode

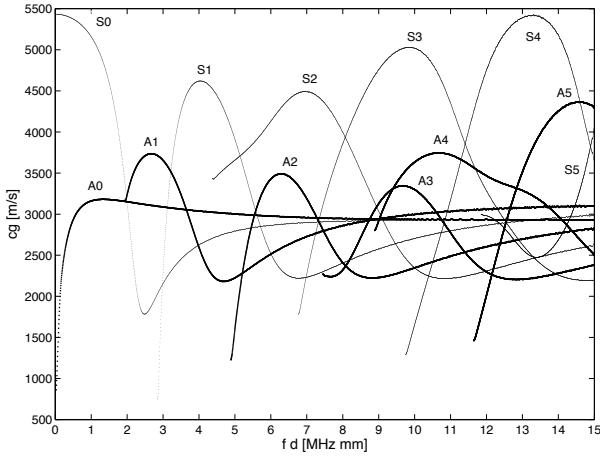


Figure 2. Dispersion curves for group velocity of Lamb waves ($C_L = 6420$ m/s i $C_T = 3040$ m/s); S - symmetric modes, A - antisymmetric modes

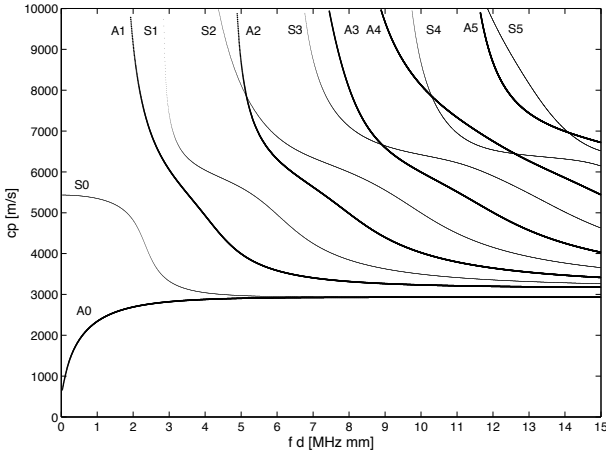


Figure 3. Dispersion curves for phase velocity of Lamb waves ($C_L = 6420$ m/s i $C_T = 3040$ m/s); S - symmetric modes, A - antisymmetric modes

simply obtained using formulas: 10, 11 for symmetric modes and formulas 12, 13 for antisymmetric modes:

$$u_S = -2k^2q \cos(qh) \cos(pz) + q(k^2 - q^2) \cos(ph) \cos(qz) \quad (10)$$

$$w_S = -2ikpq \cos(qh) \sin(pz) - ik(k^2 - q^2) \cos(ph) \sin(qz) \quad (11)$$

$$u_A = -2k^2q \sin(qh) \sin(pz) + q(k^2 - q^2) \sin(ph) \sin(qz) \quad (12)$$

$$w_A = 2ikpq \sin(qh) \cos(pz) + ik(k^2 - q^2) \sin(ph) \cos(qz) \quad (13)$$

where: d - half of plate thickness [m], z - coordinate of point in which displacement is calculated [m], i - imaginary unit.

Calculated displacement fields for both Lamb wave modes with different frequencies are presented in Figure 4.

Let's get back to the dispersion curves especially those presenting phase velocity. These dispersion curves are very useful in the case of elastic wave generation. Wave packet consists of some number of waves with frequencies from certain frequency band. Dispersion curves for phase velocities show velocities with which ingredient waves from wave packet propagate. In the case of different values of phase velocities related with ingredient waves the shape of wave packet to be changed with growing distance of waves propagation. This fact is caused by dispersion phenomenon. In order to reduce effect of dispersion excitation signal used during elastic wave generation must be characterized by narrow frequency band. To improve the result of dispersion effect reduction frequency band of excitation signal must be located in the flat part of phase velocity curve. In order to limit the span of frequencies in the excitation signal modulation windows are used. Additionally small number of cycles of sine function (usually 3 to 15) is used as excitation signal. In the Figure 5 three types of modulation window were used in order to modulation of excitation signal in the form of sine with five cycles (carrier frequency 300 kHz).

In the case of Hann window (Figure 5a,b) the narrowest frequency band will be obtained. A little bit wider frequency band will be obtained in the case of triangular window modulation (Figure 5c,d). Definitely the widest frequency band will be obtained in the case of rectangular window (Figure 5e,f). Many additional peaks around main frequency band can be observed (Figure 5f).

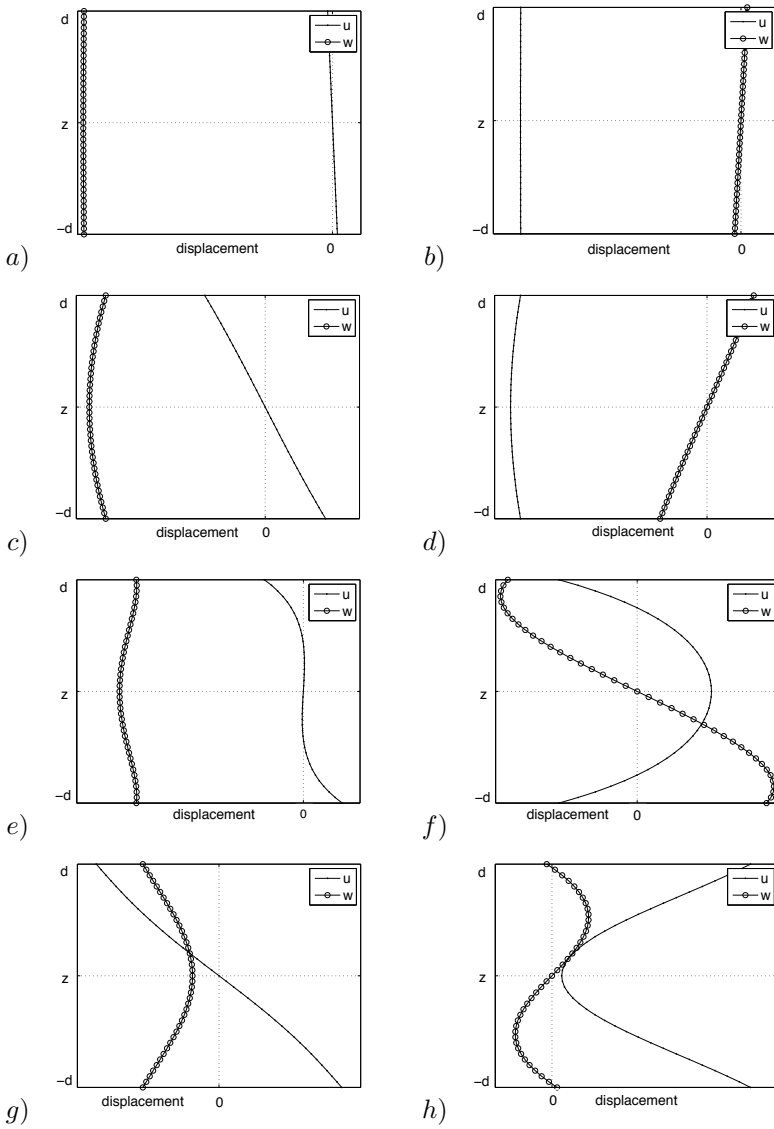


Figure 4. Distributions of in-plane (u) and out-of-plane (w) components of displacements of antisymmetric (left column) and symmetric (right column) Lamb wave modes for frequencies: a,b) 100 kHz, c,d) 250 kHz, e,f) 800 kHz, g,h) 3000 kHz

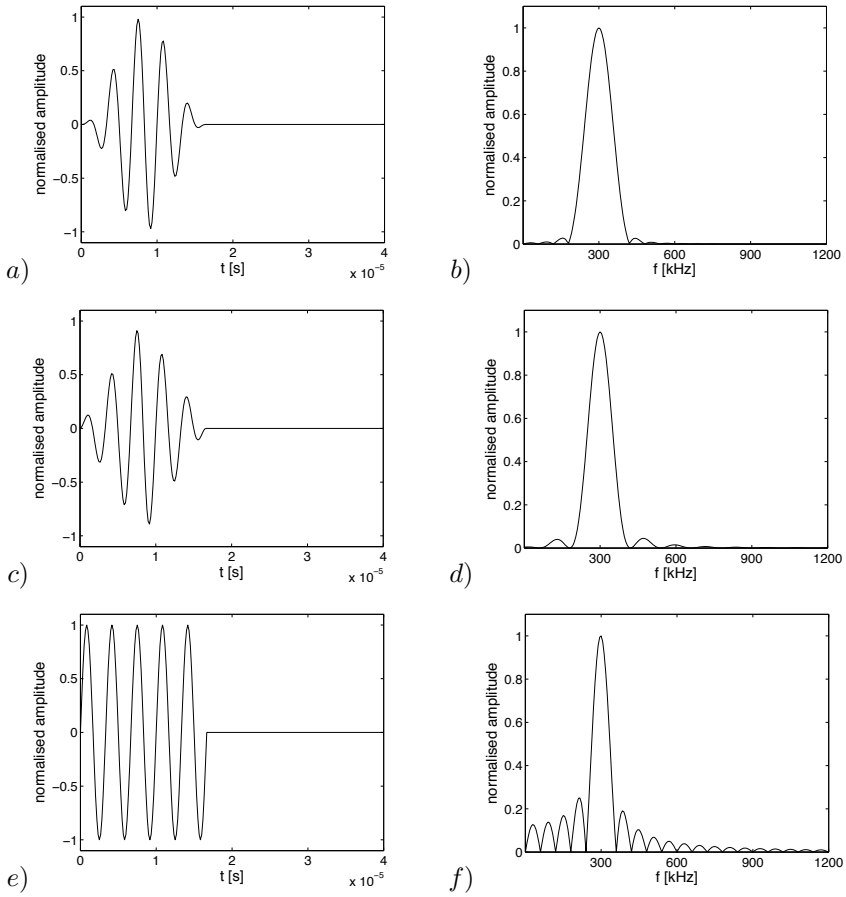


Figure 5. Different modulation types: a,b) Hann window, c,d) triangular window e,f) rectangular window. Left column - signal in time domain, right column - signal in frequency domain

3 Elastic wave generation and sensing

Many techniques can be utilized in order to excite or sense. However each of known method have some advantages and drawbacks that limit its applications. In this section a short review of various techniques for elastic wave generation and sensing will be presented.

3.1 Elastic waves generation techniques

Simplest well known method of elastic waves generation is method utilizing impulse of force. In practice impulsive character of force is realized by modal hammer or impact of steel ball (Kundu et al., 2008), (Jeong, 2001). These two methods are used during the scientific research but in the case of real structures impact can be caused for example by bird strike. In case of scientific research related with composite structures so called Hsu-Nielsen method is utilized that really on breaking the pencil lead (Berthelot et al., 1992). The common disadvantage of mentioned method is fact that impulsive character of excitation cause that wide range of frequencies are generated. This fact is very undesirable in the case of Lamb type elastic waves because wide frequency band of excitation bring about problem of dispersion phenomenon besides more than two fundamental modes of these waves will be excited. Because of mentioned restrictions new method that allow to control frequency band of excitation have been developed. Most of all ultrasonic technique is known which utilizes conventional plane bulk longitudinal wave transducers (Wilcox, 1998). These transducers are immersed in liquid (water for example) together with the structure in which elastic waves are to be generated - Figure 6. Transducer generates a longitudinal waves that propagate through the liquid.

When propagating waves reaches the structure due to internal wave reflections Lamb waves are generated in the structure. This method very often is precluded from application in many engineering structures because of need to use liquid in which transducer and structure must be immersed. Therefore instead of liquid air as a medium is used but only small part of longitudinal wave is converted into Lamb waves for this combination. This problem is caused by different acoustic impedance of air and the most of materials which is used for structural element manufacture. Problem of liquid or air usage can be eliminated by the using of ultrasonic transducers integrated with coupling material named Perspex (Plexiglas). These transducers are called wedge coupled angle-adjustable ultrasonic probes (Wilcox, 1998). Advantage of mentioned transducers it that by choosing the angle of ultrasonic transducer orientation it is possible to actively tune in order to excite chosen mode of elastic waves. Well known are also comb-type ultra-

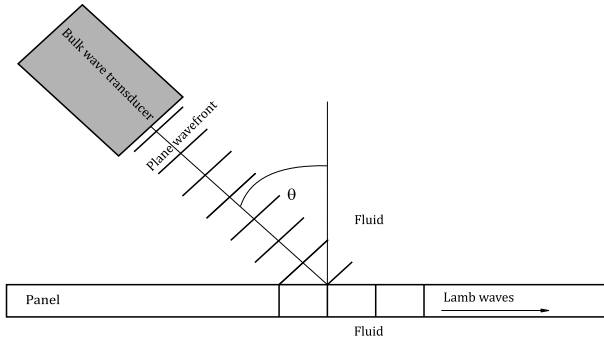


Figure 6. Idea of elastic wave generation in plate using a conventional ultrasonic transducer

sonic transducers (Rose, 2004) which scheme is presented in Figure 7. These transducers consist of some number of periodically spaced tips. Spacing of tips must correspond with length of generated wave. The main disadvantage of this transducer application is fact that tips spacing determine the specific wavelength and this is done in permanent fashion. Described methods are not used nowadays.

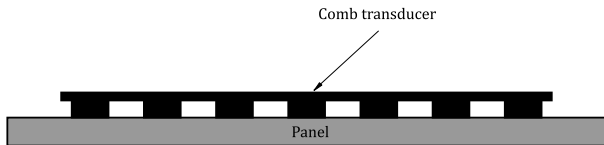


Figure 7. Scheme of comb-type ultrasonic transducer

Nowadays new methods are developed for elastic wave generation. First of such methods is based on electro-magnetic phenomenon. Transducers utilizing mentioned phenomenon are called Electro Magnetic Acoustic Transducers (EMATs) (Park et al., 2006), (Murayama and Mizutani, 2002), (Dixon and Palmer, 2004). These transducer can be used only in the case of metallic structures, moreover material of structure must be ferromagnetic. EMATs consist of fixed magnet with solenoid through which flows electrical current. As result eddy currents are induced in structure and these currents generate elastic waves. The most important disadvantage is that EMATs are very large and heavy.

The most popular transducers that are widely use for elastic wave generation are based on piezoelectric effect (Giurgiutiu, 2008), (Ihn and Chang, 2004), (Ostachowicz et al., 2009). Piezoelectric transducers are very thin, light and can be simply integrated with structure however these transducers are very fragile. Solid-state solution of two perovskities (lead titanate) and (lead zirconate) is well known as PZT. Different types of piezoelectric transducers utilized in authors laboratory are presented in Figure 8.



Figure 8. Different types of piezoelectric transducers in authors laboratory; from the left: MIDE QP22B, T216-A4NO-273X Piezo Systems, Inc., Noliac CMAP06 and Noliac CMAP11, Ceramtec Sonox P502 disc

During the elastic wave generation inverse piezoelectric effect is utilized. This effect allow to generation strain in piezoelectric materials due to external electrical field application. This effect can be described by constitutive equation 14.

$$\begin{aligned}
 \begin{pmatrix} S_{11} \\ S_{22} \\ S_{33} \\ S_{23} \\ S_{31} \\ S_{12} \end{pmatrix} &= \begin{pmatrix} s_{11} & s_{12} & s_{13} & 0 & 0 & 0 \\ s_{21} & s_{22} & s_{23} & 0 & 0 & 0 \\ s_{31} & s_{32} & s_{33} & 0 & 0 & 0 \\ 0 & 0 & 0 & s_{44} & 0 & 0 \\ 0 & 0 & 0 & 0 & s_{55} & 0 \\ 0 & 0 & 0 & 0 & 0 & s_{66} \end{pmatrix} \begin{pmatrix} T_{11} \\ T_{22} \\ T_{33} \\ T_{23} \\ T_{31} \\ T_{12} \end{pmatrix} + \\
 &+ \begin{pmatrix} g_{11} & g_{21} & g_{31} \\ g_{12} & g_{22} & g_{32} \\ g_{13} & g_{23} & g_{33} \\ g_{14} & g_{24} & g_{34} \\ g_{15} & g_{25} & g_{35} \\ g_{16} & g_{26} & g_{36} \end{pmatrix} \begin{pmatrix} E_1 \\ E_2 \\ E_3 \end{pmatrix} \tag{14}
 \end{aligned}$$

where: S - strains [-], s - compliance coefficients [m^2/N], T - stresses [N/m^2], d - piezoelectric coupling coefficients for strain-charge form [C/N],

E - electric field [N/C].

In order to protect piezoelectric transducers from aggressive environment and humidity a special layers were developed. Such a layers were made out the polyamide foil in which transducers were embedded. Such a commercial solution is known as SMART Layer (Stanford Multi-Actuator-Receiver Transduction Layer) and was developed in Stanford University and produced by Acellent Technologies, Inc. (Lin and Chang, 2002), (Qing et al., 2009), (Qing et al., 2006). Very similar to them is solution named SAL (Smart Active Layer) developed in Korea Research Institute of Standards and Science (Lee et al., 2005).

Elastic wave are also generates using inter-digital transducers (IDT) (Mustapha et al., 2007) they are very similar to ultrasonic comb transducers (Figure 9, 10). IDT transducers very often are made of PVDF (polyvinylidene fluoride) which has very important advantage - is very flexible. Thanks to this it can be simply integrated with curved shape structures like pipes, tanks, shells, etc.

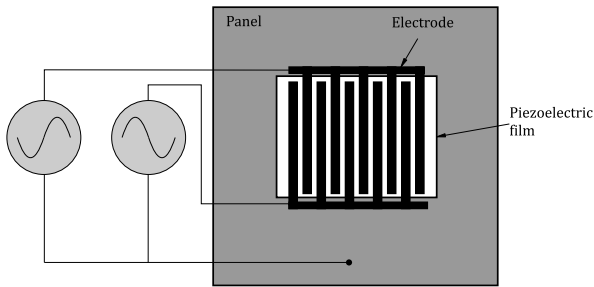


Figure 9. Scheme of inter-digital transducer IDT - top view

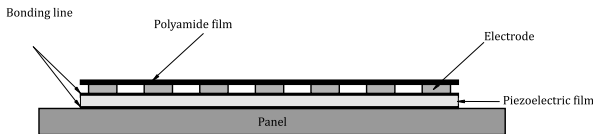


Figure 10. Scheme of inter-digital transducer IDT - side view

A little bit similar solution are MFC (Macro Fibre Composite) (Wagg et al., 2007) and APC (Active Fibre Composite) ((Melnikowycz et al., 2006) and (Melnikowycz et al., 2010)) transducers made of piezoelectric fibres embedded into the foil (Figure 11). The only one difference in these transducers

are cross-section of fibres: square in the case of MFC and circular for AFC. Both types are also very flexible like in the case of IDT transducers.

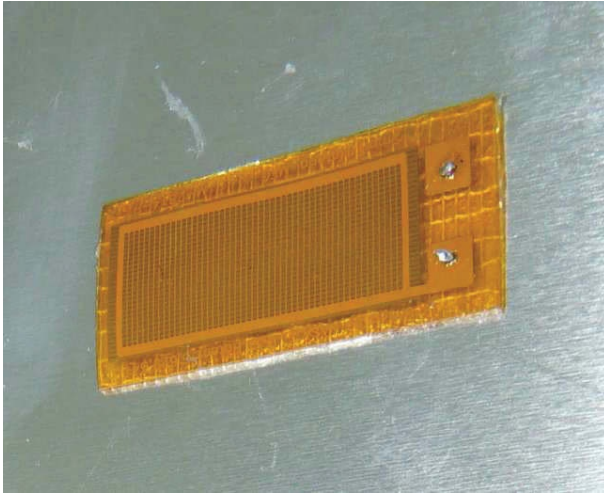


Figure 11. Macro Fibre Composite (MFC) transducer in authors laboratory

It also should be mentioned that magnetostrictive effect can be utilized for elastic wave generation. Transducers employing this effect consist of fixed magnets, solenoids and nickel gratings. These transducers are able to excite high-power elastic wave. Besides this type of transducers can be used in the case of non-ferromagnetic materials. Elastic wave can be also excited using photo-thermal non contact methods. In this approach Nd:YAG laser sources is used for elastic wave excitation (Valle and Little, 2002), (Hongjoon et al., 2006a), (Hongjoon et al., 2006b). Main advantage of this approach is the possibility of generation of waves with chosen shape of source and in chosen site of structures.

3.2 Elastic waves sensing techniques

Apart from elastic waves generation such a same important is the process of elastic wave sensing and visualization of its propagation in the structures. Similarly like in the case of elastic waves generation in the case of sensing many techniques can be distinguished. Some of them are the same for both cases but few methods can be only utilized in the purpose of wave sensing. In the past, very often for elastic wave sensing conventional plane bulk longi-

tudinal wave transducers were used however wedge coupled angle-adjustable ultrasonic transducers, comb-type ultrasonic transducers were also commonly used. In order to sense elastic waves until now transducers leveraging magnetic phenomenon (EMATs) are used. This type of transducer was described in previous section. At present very interesting is method that is based on piezoelectric transducers. During the elastic wave sensing direct piezoelectric effect is utilized. As result of transducer mechanical deformations electrical charges appear on the electrodes of piezoelectric element. Direct piezoelectric effect can be described using constitutive equation 15.

$$\begin{aligned} \begin{Bmatrix} D_1 \\ D_2 \\ D_3 \end{Bmatrix} &= \begin{Bmatrix} g_{11} & g_{12} & g_{13} & g_{14} & g_{15} & g_{16} \\ g_{21} & g_{22} & g_{23} & g_{24} & g_{25} & g_{26} \\ g_{31} & g_{32} & g_{33} & g_{34} & g_{35} & g_{36} \end{Bmatrix} \begin{Bmatrix} T_{11} \\ T_{22} \\ T_{33} \\ T_{23} \\ T_{31} \\ T_{12} \end{Bmatrix} + \\ &+ \begin{Bmatrix} \epsilon_{11} & \epsilon_{12} & \epsilon_{13} \\ \epsilon_{21} & \epsilon_{22} & \epsilon_{23} \\ \epsilon_{31} & \epsilon_{32} & \epsilon_{33} \end{Bmatrix} \begin{Bmatrix} E_1 \\ E_2 \\ E_3 \end{Bmatrix} \end{aligned} \quad (15)$$

where: D - charge-density displacement [C/m^2], ϵ - electric permittivity [F/m].

In the Figure 12 some real application of piezoelectric transducer network is presented. In this case piezoelectric transducers are used for excitation and sensing of elastic wave propagation during the fatigue test of the part of helicopter main rotor blade. During the fatigue tests crack was propagating from the previously introduced notch - Figure 13.

Likewise in the case of elastic wave excitation for sensing purpose elastic SMART Layers are used as well as pure PVDF material, inter-digital transducers IDT and transducers based on piezoelectric fibres laminated in polyamide film: Macro Fibre Composites MFC and Active Fibre Composites AFC. Very interesting is method based on paint with piezoelectric properties. This paint can be simply sprayed on the structural element. The main disadvantage of this method is the low sensitivity.

In the case of elastic waves registration also magnetostrictive transducers are used that were described in previous subsection. Some method allow only to register elastic waves without possibility of its excitation. These methods are based on optical phenomena. In 1864 August Toepler developed a method for visualisation of flows with variable density. This method was called schlieren photography. Optical system that is used in this method includes collimated light source illuminating a flowing fluid. Changes of



Figure 12. Elastic wave propagation measurements in the part of helicopter main rotor blade during the fatigue tests

refraction index resulting from fluid density gradient have influence on the collimated light beam. In results spatial changes of light intensity that in turn allow to visualise phenomena in the fluid flow. This technique allowed to determine velocity of ultrasonic wave propagation in solids. Such a experiments were conducted by Barnes and Burton in 1949, Chinnery, Humphrey and Beckett in 1997, and Neubauer in 1973 (Rose, 2004). Some theoretical work on visualisation of elastic wave propagation was also performed in 1922 by Brillouin. He investigated interactions between elastic waves in solids and electromagnetic waves. These interactions can be noticed as a changes of medium permittivity due to elastic wave propagation. Experimental research for this topic was done by Lucas and Biquard in France and



Figure 13. Growing crack in the part of helicopter main rotor blade during the fatigue tests - back side view

Debye and Sears in the US (Royer and Dieulesaint, 1999). Later the same topic was investigated by Raman and Nath in India (Royer and Dieulesaint, 1999).

Very interesting technique for visualisation of elastic wave propagation is photoelasticity method. Mentioned method can be used for visualisation of propagating elastic waves in glass. This method is based on fact that polarised light can be divided into the components that propagating with different velocities. As result colourful fringes associated with deformations of material can be observed. Photoelasticity method can be used in materials exhibiting birefringence resulting from material stress. As result of birefringence material to exhibits distinct refractive indexes. Value of refractive index at given point of material is strictly correlated with level of mechanical stress. Described method was used for ultrasonic waves visualisation by Zhang, Shen and Ying (1988) and by Li and Negishi (1994) (Rose, 2004).

In recent years new techniques are being developed for elastic wave registration. One of the newly developed method is based on polarimetric fibre optic sensors and fibre Bragg grating sensors (FBG) (Thursby et al., 2004). Polarimetric sensors require simple equipment for elastic wave sensing however registered signals are very difficult in interpretation and analysis. In the case of FBG sensors more complicated equipment must be used but measurements are easy to interpret. Polarimetric sensors allow to take

measurements from larger area of structure than in the case where FBG sensors are used. The great advantage of using FBG sensors is its multiplexing capability. One measurement set-up can be used for generating and registering optical signal for the grid of sensors. The most important thing in the field of elastic wave sensing is that the length of fibre optic sensor must be at least seven times shorter than the length of elastic wave being sensed (Takeda et al., 2005). Fibre optics sensor are very light, have very small diameter however they are very brittle like a piezoceramic materials. Due to new technological achievements in optics-based measurement technologies non-contact optical techniques came back. First widely used method for visualisation of elastic wave propagation is shearography method. This method is non-contact deformation measurement technique that is based on laser source and image shearing camera. This camera is used to create pair of laterally shifted images. Laser source is used for illumination of structure being measured. As result shifted images interfere creating such a called speckle image. In the purpose of elastic wave sensing a combination of spatial phase shifting technique and shearography is used. This can be achieved using Mach-Zehnder interferometer. Very often for elastic wave sensing Electronic Speckle Pattern Interferometry (ESPI) method is used (Lammering, 2010).

In recent years more and more significant is method based on non contact laser vibrometer. Operational principle of laser vibrometer is based on Doppler effect. Laser vibrometer register changes in frequency of light beam reflecting from vibrating surface of measured structure. Single point vibrometers are equipped with one measurement head (1D) and allow to measure velocity of chosen point of vibrating structures along the direction of laser beam. In order to measure vibrations in few point laser head must be manually positioned. Scanning vibrometer allow to scan the vibration of structures in chosen points. Laser beam is directed to chosen point of mesh using set of mirrors controlled by system. In some cases information on vibration in three dimensions are important therefore 3D scanning laser vibrometer has been developed. This equipment consists of three independent laser measurement heads (Figure 14). These measurement heads are oriented at different angles relative to structure being measured. Three laser beams must be focused in one points. Before the vibration measurement system measure the geometry of structure. Knowing the structure geometry and positions of measurement heads system simply can measure components of vibration velocities and as result compose full vector of vibration velocity in chosen point of structures. Due to scanning feature of vibrometer vibration velocities for whole structure surface can be simply extracted.



Figure 14. Measurement heads of Polytec PSV-400 3D scanning laser vibrometer

The main advantage of laser vibrometry techniques is non contact measurement approach. Non contact measurement eliminate problem related to additional mass of sensors attached to the structure and the problem of contact sensor with structure. This is especially very important problem during the measurements of elastic wave propagation. Any additional mass like a transducers cause a changes of elastic wave propagation (wave reflections) and disturb the measurements. Laser vibrometer is very useful during the experimental research in laboratory or during the outdoor measurements but it cannot be utilized in real time SHM systems.

Now some experimental result will be presented related to 3D laser vibrometry technique utilized for elastic waves sensing. First example is related with measurement of three components of displacement (two in-plane and one out-of-plane) connected with elastic wave propagation in plate made out of EN AW-5754 aluminium alloy. Carrier frequency of excitation was equal 200 kHz . These components of displacement were measured in one point and are presented in Figure 15.

Second example is connected with visualisation of elastic wave propagation also in plate made out aluminium alloy. Displacement filed were measured in the mesh of points covering whole surface of plate. Excitation carrier frequency was equal 100 kHz . Results of measurements are

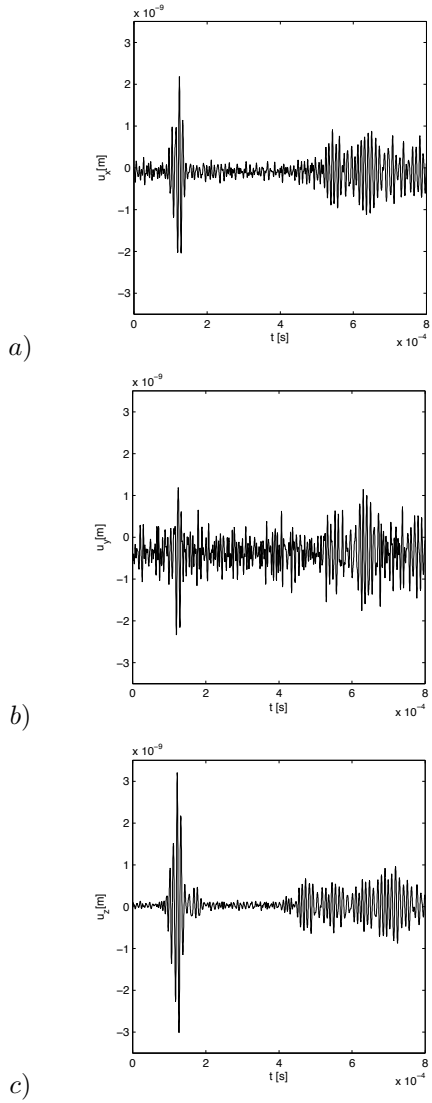


Figure 15. Measured three components of displacements in one point using 3D laser scanning vibrometer: a) in-plane x component, b) in-plane y component, c) out-of-plane z component

presented in Figure 16. Visualisation of in-plane and out-of-plane displacement components allow to understand better the phenomenon of Lamb wave propagation especially in structures with complicated geometry. Even in the case of so simple structure like plate 3D scanning measurements are very helpful because symmetric and anti-symmetric modes can be easily noticed. Both of these modes can be observed for the in-plane components Figure 16a,b) but symmetric mode (larger wavelength) has larger amplitudes. Anti-symmetric mode can be observed for the out-of-plane displacement component Figure 16c).

Last example is connected with visualisation of elastic wave propagation in the part of helicopter main rotor blade with crack. Measurement equipment and specimen are presented in Figure 17. In this case only out-of-plane displacements were measured. Results of elastic wave propagation are presented in the Figure 18.

4 Wave generation and sensing equipment

In this section examples of equipment for elastic wave generation and sensing are presented. It should be emphasized that all presented equipment is connected with piezoelectric transducers. The simplest way of elastic wave excitation and sensing can be realised using popular laboratory equipment like digital signal generator, oscilloscope and some equipment dedicated for piezoelectric transducers (Figure 19). Digital signal generator also called arbitrary waveform generator allow to define signal parameters (frequency, type of modulation, voltage) and generate signal that will drive piezoelectric transducers. Signal before to be driven piezoelectric transducer have to be amplified. For this purpose amplifier especially dedicated to piezoelectric transducer has to be used (capacitive electrical load). In the authors laboratory EPA-104 Piezo Linear amplifier produced by Piezo System, Inc. is used (Figure 19b). The last one is the digital oscilloscope used in order to register signal from piezoelectric transducers. It should be underlined that electrical signal from piezoelectric transducers can only be registered directly by oscilloscope if the transducer have large capacitance. In the case of very small capacitance of piezoelectric transducer additionally dedicated charge amplifiers should be used.

In practice better way is to use compact measurement equipment that allow to generate and sense signals. It is especially very important during the measurements conducted outside the laboratory. Therefore authors have designed compact equipment for this purpose, see Figure 20. This equipment allow to generate in one chosen channel from thirteen accessible channels and to register signals in the rest twelve. This equipment is con-

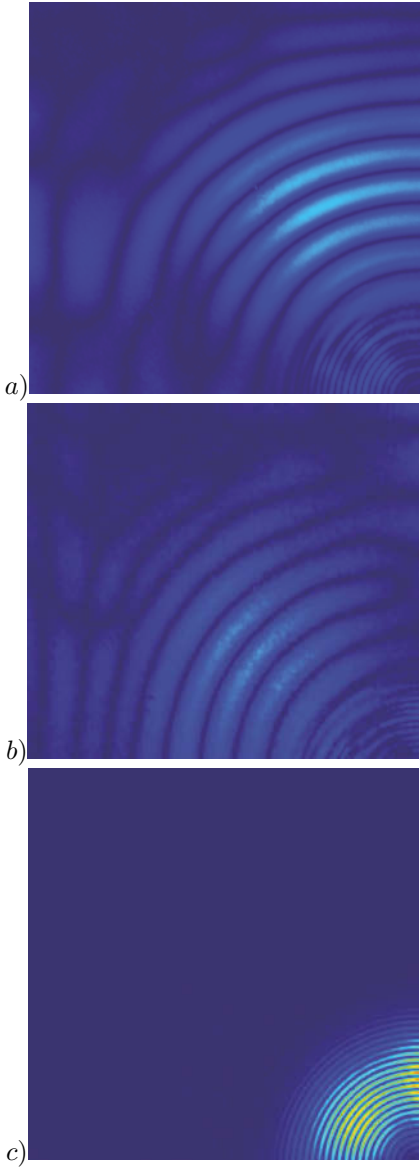


Figure 16. Visualisation of elastic wave propagation (displacements): a) in-plane x component, b) in-plane y component, c) out-of-plane z component



Figure 17. Measurements of elastic wave propagation in the part of helicopter main rotor blade using laser vibrometer

trolled by computer using MATLAB environment. Control software allow to set such a parameters as a channel for excitation, channels for registration, voltage of excitation, number of cycles of tone-burst excitation signal and modulation type.

Very interesting is also commercial compact system produced by Acellent Technologies, Inc. (Figure 21).

5 Transducer network configurations

In SHM systems very often piezoelectric transducers are utilized for elastic waves generation and sensing. Single piezoelectric transducers are arranged

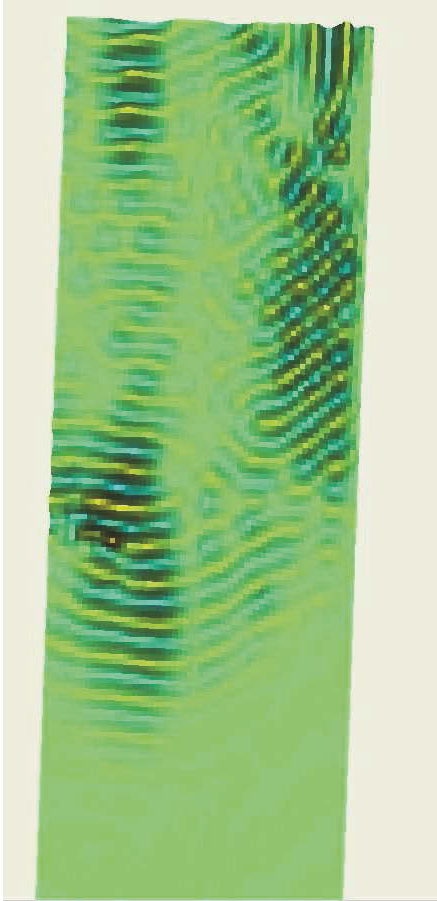


Figure 18. Visualisation of elastic wave propagation in part of helicopter main rotor blade with crack

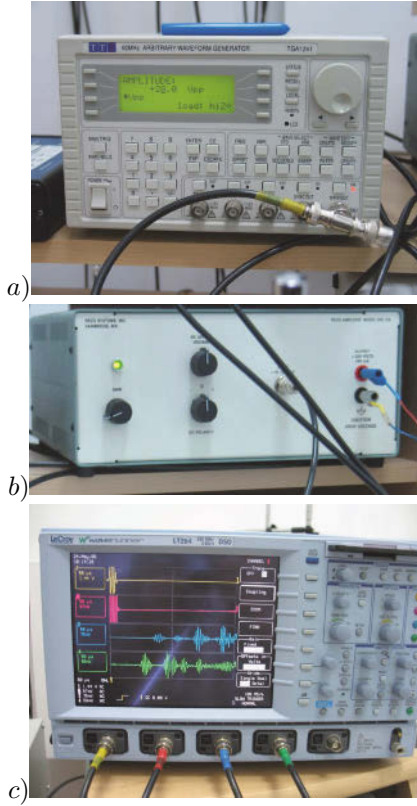


Figure 19. Simplest laboratory measurement equipment: a) digital signal generator, b) piezo amplifier, c) oscilloscope

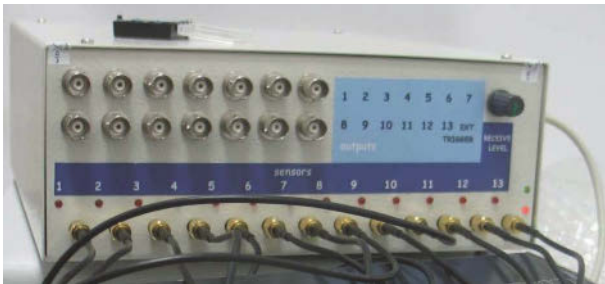


Figure 20. Propotype for elastic wave generation and sensing



Figure 21. Elastic wave generation and sensing system available on the market

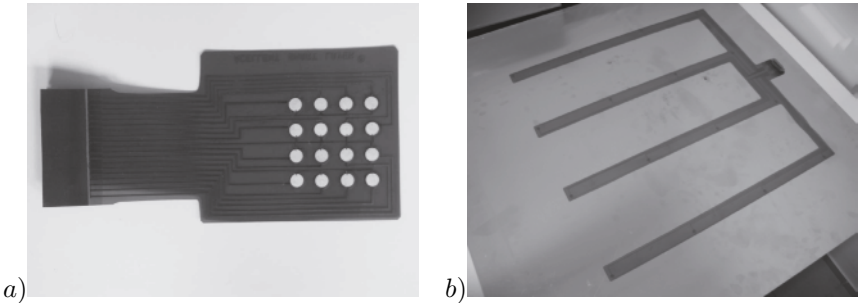


Figure 22. Piezoelectric transducer configurations in authors laboratory: a) concentrated, b) distributed

in network with various configurations. Generally three types of network configurations can be distinguished: concentrated (Giurgiutiu, 2008), distributed (Ihn and Chang, 2004), mixed (Malinowski et al., 2011). In the first case transducers are placed close to each other in chosen site of structure (Figure 22a). In the case of distributed network transducers are placed uniformly (or not) on the surface of the structure (Figure 22b). In the case of mixed configuration network consists of uniformly (or not) placed group of transducers. In each part transducers are placed close to each other.

Type of transducer network configuration and manner of transducer

placement depends on method of elastic wave generation and sensing that is used. Three methods of elastic wave generation and sensing can be distinguished from the literature: pitch-catch, pulse-echo and phased array. In the pitch-catch method elastic waves are excited in one transducer and sensed in the second. If elastic wave propagates through the damaged area its amplitude decrease and propagation velocity of wave is changed. Such a method can be utilized with distributed or mixed transducer networks. In the pulse-echo method elastic waves are generated in one transducer. Elastic wave propagating in the structure reflects from damage and these reflections are sensed in second (or the same) transducer. This method can be used with concentrated or mixed transducer network. Phased array method is based on constructive elastic wave interference phenomenon. As result of firing transducers in concentrated network with specially adjusted time delay wave front is created that propagate in chosen direction. This method works like airborne radar. In this method wave reflections are amplified and thank to this damage placed far away in relation to transducers can be localised. Very important is assumption that distance between two neighbour transducers must be less or equal half of wavelength. It should be mentioned that this method can be also utilized with mixed transducers network. But in this case it will be combination of few individual phased array systems for each concentrated transducer subgroup from whole configuration.

The next two sections contain description of damage localisation algorithms that are used in Structural Health Monitoring application. The theoretical background is followed by examples based on experimental measurements. The experimental investigation was conducted in author's laboratory. Both concentrated and distributed transducer arrays were considered. Provided examples cover the case of an aluminium alloy panel and a CFRP panel.

6 Energy summing algorithm

6.1 Basis for numerical algorithm

In this approach it is assumed that any discontinuity on the elastic wave propagation path causes wave reflection. In the general approach the sensing configuration consists of N transducers that excite and sense elastic waves. In order to monitor a surface with these transducers they are placed in special manner in points $T_i (i = 1, \dots, N)$. The transducer placement is not important at this point. For simplicity of explanation but without losing the generality a flat surface is assumed. In order to obtain information from a point P arbitrarily chosen from the surface the following distances

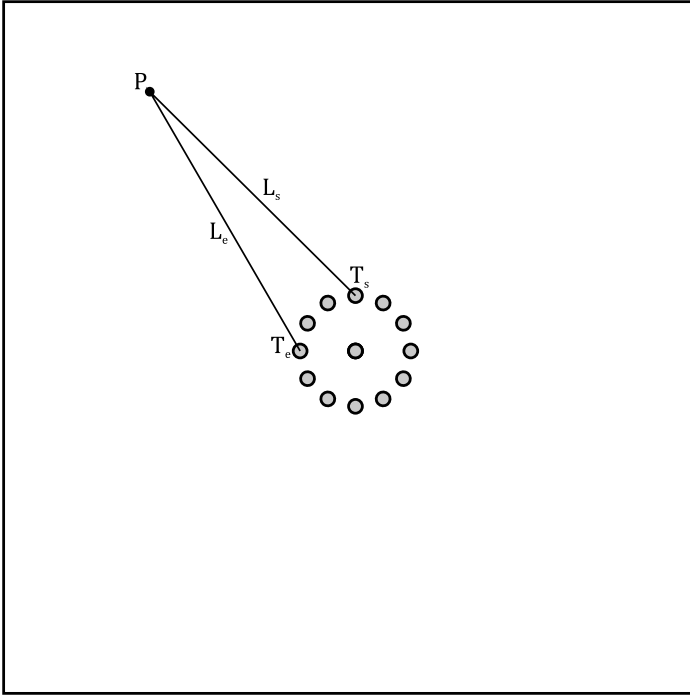


Figure 23. An example indicating transducer placement and distances needed for calculations.

are calculated (Figure 23)

$$\begin{aligned} L_e &= |T_e P|, \\ L_s &= |T_s P|. \end{aligned} \tag{16}$$

If the time of wave generation and the time of starting wave sensing is the same, the wave should be sensed in transducer T_s after the time:

$$t = \frac{L_e + L_s}{c} \tag{17}$$

where c is group velocity of wave propagation. Beginning at time instant t , segments of signals recorded in transducer T_s are extracted (Figure 24). Time width of this time segment is denoted by Δt . This segment is denoted by B_k , where k is an index ($k = 1, \dots, K$). Damage indicator associated

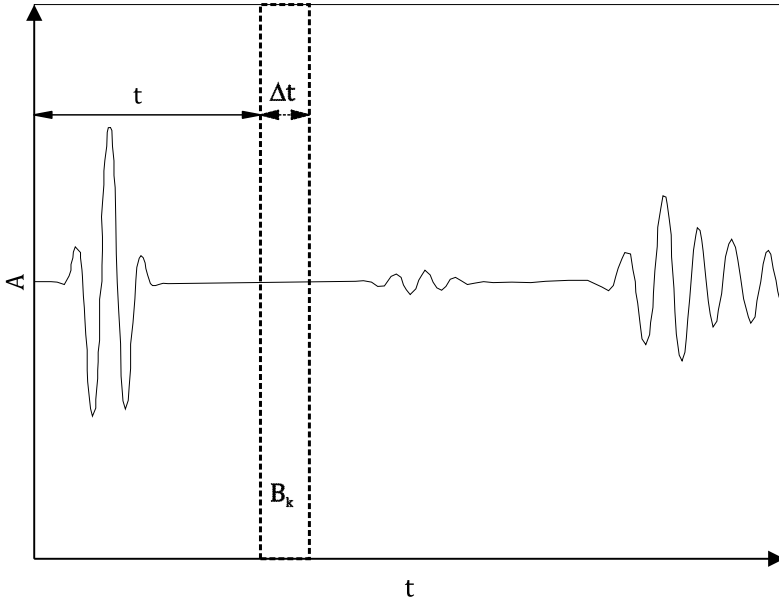


Figure 24. Illustration of signal segment extraction for creating a damage index.

with point P and based on two transducers (T_e, T_s) is defined as

$$DI(P) = \sum_{k=1}^K (D_k B_k)^2 \tag{18}$$

where D_k is a compensating coefficient taking into account amplitude decay with travelled distance.

The more general formula can be written if one consider all sensors. In this case two additional sums are needed. First for sensing and second for excitation transducers:

$$DI(P) = \sum_{i=1}^N \sum_{j=1}^N \sum_{k=1}^K (D_{ijk} B_{ijk})^2 \tag{19}$$

If the extracted segments contain reflected waves, value of the indicator DI for point P will be larger than for other points. This will clearly indicate a potentially damaged area. The procedure described above is repeated for other points of the monitored area.

Similar approach of mapping information contained in signals is based on adding either values of signal amplitudes or envelopes for a single time sample corresponding to a point within the monitored area. This means that for the DI only the time sample (or its envelope) corresponding to t is extracted (Michaels et al., 2008).

Another approach for damage localisation can use the information from the frequency domain. Damage localisation is preformed by exciting a structure with a known signal with frequency f_0 . This signal is applied to the transducer electrodes. The frequency spectrum of such signal is known or can be calculated. Due to dispersive nature of elastic guided waves very often the excitation signal is chosen in the form of tone burst with energy concentrated in relatively narrow frequency band around f_0 . And, this information can be used for creating the damage index. The procedure is following:

1. Perform the Fast Fourier Transformation on signal segments B_{ijk} .
2. Extract the amplitude value from FFT module for carrier frequency f_0 and denote it by B_{ijk}^f
3. Create new damage index

$$DI_f(P) = \sum_{i=1}^N \sum_{j=1}^N B_{ijk}^f \quad (20)$$

By analogy, the obtained frequency damage index DI_f is associated with point P . The procedure described above is repeated for other points of the monitored area. By its definition, the frequency damage index is a frequency filter. Extraction of the frequency response for f_0 guarantees that damage index is not influenced by measurement noise with other frequencies.

The results of the described algorithm in the form of damage index DI are aligned along an ellipsis with foci in the exciting and receiving transducers. Of course, if the same transducers is used for excitation and sensing the ellipsis is a circle. Considering, for example, three transducers - one for excitation (T_e) and two for sensing (T_{s1} and T_{s2}) one can obtain two ellipses (Figure 25) related to higher DI . This will happen in case if there is damage in point P . For only one pair of transducers (T_e and T_{s1}) the result is ambiguous and equal DI is obtained along the ellipsis. When an additional signal for signal processing is used (from transducer T_{s2}) there are four points of ellipsis intersection at which DI increases. One is the correct point P and the remaining intersections are denoted by P' (Figure 25). This means that the result is more precise - only four possible indications of damage. Adding more transducers results in intersection of more ellipses and the result become unambiguous.

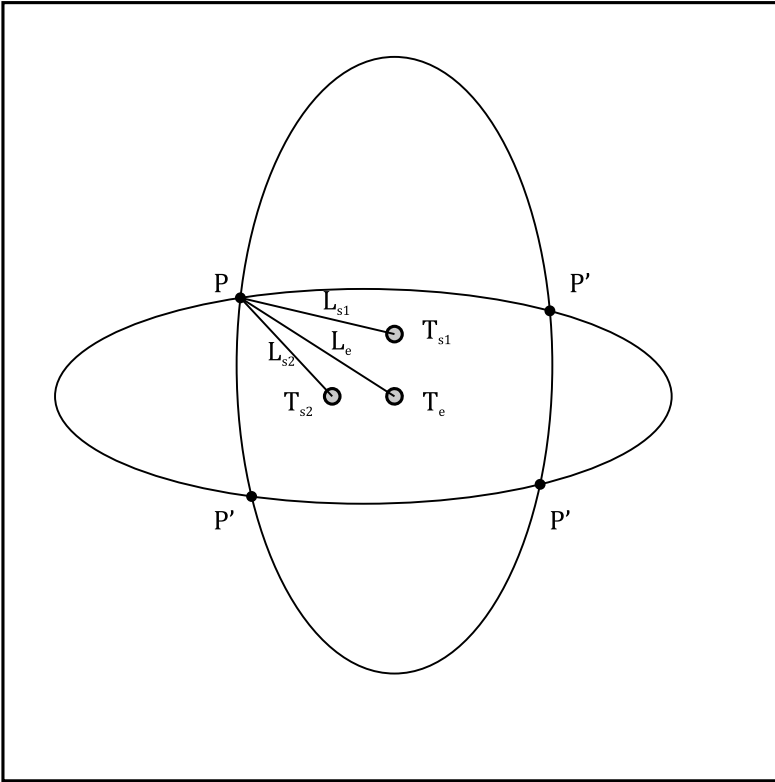


Figure 25. Illustration of the signal processing result.

6.2 Results

Concentrated configuration The described algorithm was applied to results of experimental investigation. Aluminium panel with dimensions of $1000 \text{ mm} \times 1000 \text{ mm} \times 1 \text{ mm}$ was considered (Figure 26). Piezoelectric transducer with diameter of 10 mm and 0.5 mm thickness was used for exciting the elastic waves. It was attached at the centre of the panel surface. For adhesion a acceloremter wax was used. Additional mass was installed on panel surface 40 mm above and 250 mm to the right from the transducer (Figure 26). Excitation signal was in the form of tone burst with frequency 16.5 kHz and 5 periods. Hann window was used for modulation. Such excitation signal was chosen due to dispersive nature of Lamb waves. Thier velocity of propagation highly depends on frequency. The perfect situation

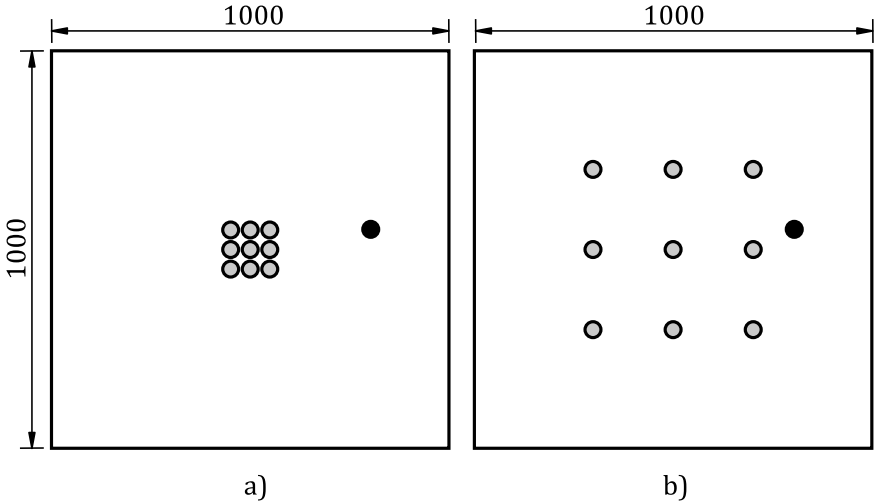


Figure 26. Aluminium panel with two types of investigated transducer configurations: a) concentrated, b) distributed. Black dot indicates the position of additional mass.

is an excitation of one frequency only, then it propagates with a defined velocity. However if a finite-length signal is considered the bandwidth gets wider. This is the reason why signal modulation is used to limit the excitation bandwidth and reduce wave dispersion.

Signals were measured by a contactless technique based on laser scanning vibrometer. The response was measured on the other side of the specimen (not this one with attached transducer). Measurement points were defined in a way to form a shape of a transducer configuration. The central point of configuration was assumed to correspond to coordinates of piezoelectric transducer. Signals measured in these points represent changes of surface vibration velocity as function of time. Both concentrated and distributed square configurations were considered that comprise of 9 elements (Figure 26). Circular grid of angular spacing between points (P) of 2° and radial spacing of 1 mm was chosen for result visualisation. Uniform method of presenting results was chosen for all damage localization methods, by representing damage indicator using colour scale mapped on the surface of the investigated element. The maximum damage value colour is white. The minimum value was presented in black. 256 levels of grey were chosen for presenting intermediate values. Images presented according to these condi-

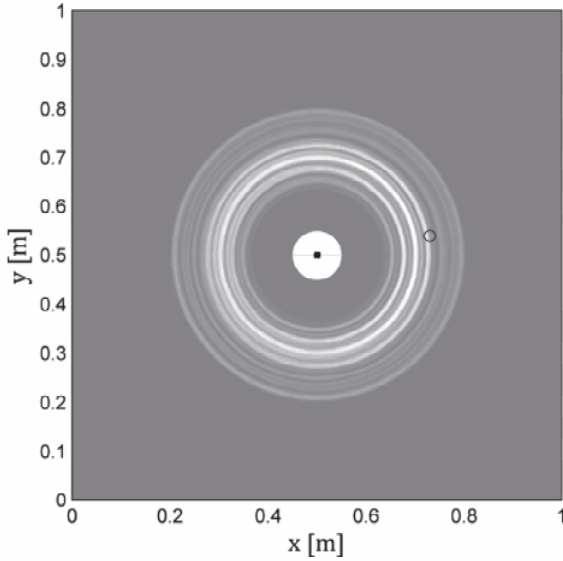


Figure 27. Localisation result for square 3×3 configuration with transducer spacing $s=3$ mm.

tions map damage indicator values onto specimen coordinates.

Concentrated square transducer configuration with 3 mm spacing was chosen as the first example. The value of damage indicator is visualised by damage influence map presented in Figure 27. Significant increases of damage indicator is visible in the form of white circle. Radius of this circle corresponds to distance from the centre of the configuration (piezoelectric transducer) to location of sought discontinuity. However, from the obtained result it is not clear where the wave reflection source lies exactly. One obtains only the radial position. Considering the diagnostic classification terminology the damage detection stage was obtained. Nevertheless, damage localization would be more useful and it was not achieved. In the course of further research the same concentrated layout ($N=9$) was tested for larger spacing of measurement points (30 mm). Result of damage localization can be seen in Figure 28. Comparing it to the result presented in Figure 27, one notices wider area with elevated damage indicator values. In the previous case these foci were located so close together that the indication was practically a circle. Increasing distance d results in more clear appearance of elliptic

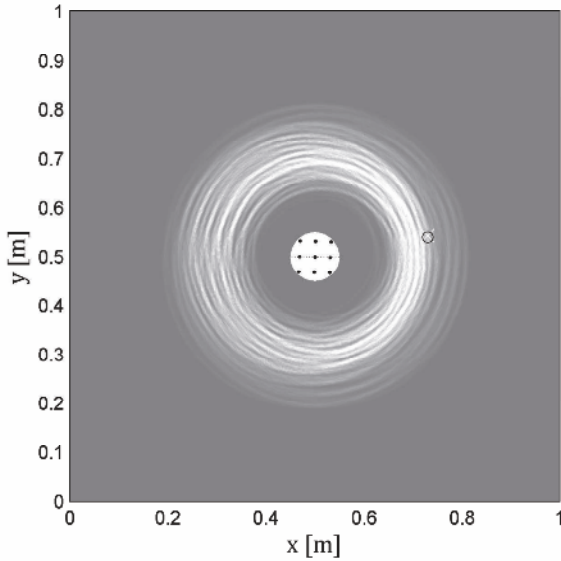


Figure 28. Localisation result for square 3×3 configuration with transducer spacing $s=30$ mm.

shapes.

In examples presented until now only nine signals were taken for signal processing because nine element arrays were considered with one source of wave excitation. It is interesting to investigate the result of adding more information (signals) to the damage detection algorithm. In order to conduct such test the 3×3 configuration has to be extended by more sensors. To keep the symmetry in relation to the piezoelectric transducer, the new configuration was chosen as an 5×5 array. This means that 16 more signals were considered in comparison to the nine-element configuration. The first investigated example was with 3 mm-long spacing so the length of the configuration edge is 12 mm-long, that is two times longer than for 3×3 configuration. The result of the localisation is depicted in Figure 29. The *DI* increase due to damage reflections is more significant in this case than for the smaller configuration (Figure 27). In order to consider a 25-element configuration of the same size as the one presented in Figure 28 the spacing needs to be set to 15 mm. The result for this case is presented in Figure 30. Characteristic elliptical shapes are visible. Sum of these ellipses around

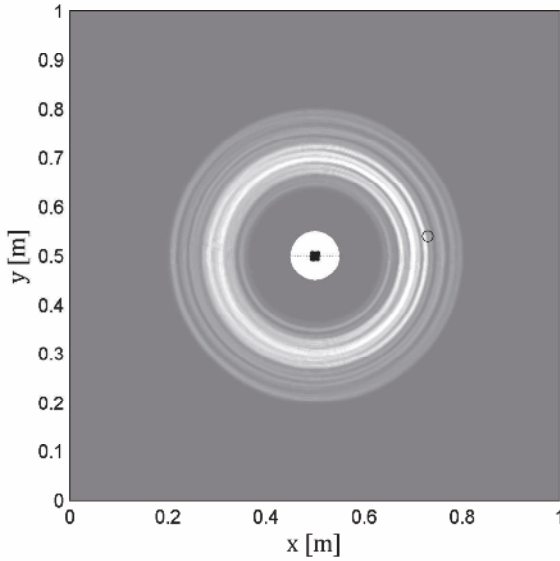


Figure 29. Localisation result for square 5×5 configuration with transducer spacing $s = 3$ mm.

the sought discontinuity (additional mass position) results in large area of high DI value. After increasing the size of configuration even more to obtain 120 mm-long edge (30 mm-long spacing) one can observe more precise result (Figure 31). The ellipses intersect in the area near additional mass. Damage index at the opposite side of the sensor configuration did not give a focused response.

Distributed configuration A concurrent solution for damage localisation is based on sparse sensor arrays forming a distributed configuration. Just like in Figure 26b). In comparison to concentrated configuration the distributed one has a potential advantage. Assuming that damage is placed far away from the concentrated arrays the distance from the sensors to damage is comparable. In the case of small damage wave reflection can be weak and the returning wave, that is registered by sensors, can be buried in signal noise. As far as distributed configurations are concerned there is a greater probability that at least one of the sensors can register the damage-related response higher than the noise level.

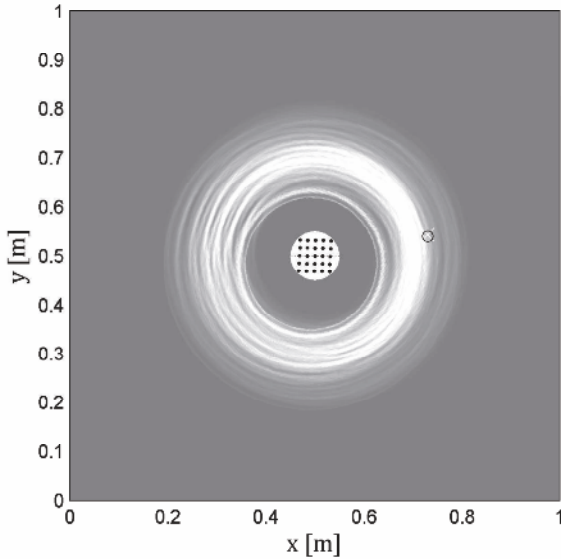


Figure 30. Localisation result for square 5×5 configuration with transducer spacing $s = 15$ mm.

In this investigation a distributed array comprising of nine sensors was taken into consideration. As previously the middle point was collocated with transducer being the source of waves. Large sensor spacing was chosen equal to 163 mm. This means that the edge of the configuration was 326 mm-long. Damage localisation result is presented in Figure 32. Characteristic ellipses can be seen. Their foci lie in the transducers position and at each sensing point. The point of intersection of the ellipses is more obvious than in the case of concentrated arrays. This intersection results in higher *DI* value that lies near the true position of the additional mass.

Test case - multi-site damage The usefulness of the energy summing algorithm was shown on the basis of vibrometer measurement. In this subsection the focus was on a more complicated case. More than one defect was considered. Research reported in this subsection was focused on square arrays used for four defects localization. The arrays consisted of nine sensors. Spacing between centres of these elements was equal to 5 mm. Middle sensor of the array was used for Lamb wave excitation. Remaining eight

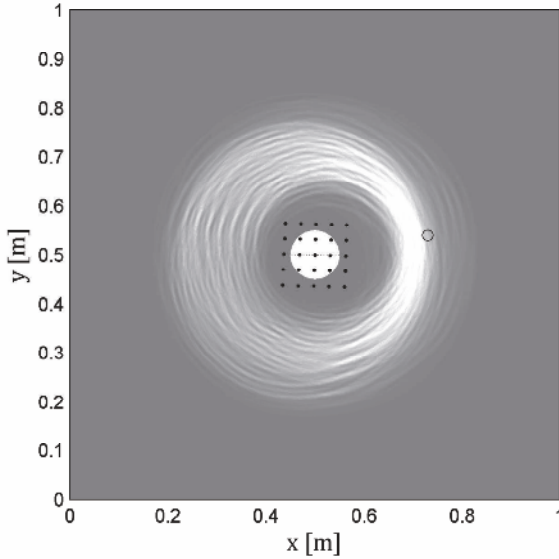


Figure 31. Localisation result for square 5×5 configuration with transducer spacing $s = 30$ mm.

was registering propagating waves. The dimensions of the sensors were following: $3 \times 3 \times 2$ mm³. Again investigation were performed on aluminium alloy AA5754 panel (1000 mm \times 1000 mm \times 1 mm). Damage was simulated in the panel by drilling two through thickness holes (Φ 6) and introducing two shallow notches, one 10 mm long and second 184 mm long. The notches were 0.2 mm wide. Considered arrays were attached to the panel in such way that the middle sensor of each array was at the centre of the panel. In order to ensure high sensitivity to small defects a relatively high frequency waves were used. The excitation frequency was chosen equal to 220 kHz. Results are showed in Figure 33. Information about damage presence was obtained. Moreover partial localisation was achieved because the radii on which the defects lie were found. In order to obtain complete localization an angular prediction is necessary. It was not achieved in this case.

6.3 Summary

In this section an experimental study was described. Its main goal was to present energy summing algorithm. This special numerical algorithm

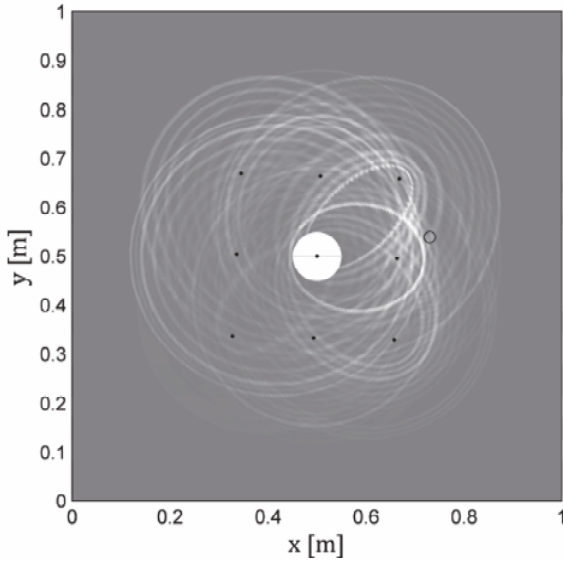


Figure 32. Localisation result for square distributed configuration with transducer spacing $s = 163$ mm.

was used to process signals gathered by the sensors and to perform damage detection. The energy summing algorithm is a very useful approach in Structural Health Monitoring. It can be applied to any sensor arrays either concentrated or distributed.

In the investigation laser vibrometer measurement points and piezoelectric transducers were used as sensors. The influence of sensor array parameters on damage localization result was investigated. The results were compared. In particular it was shown that increase in the sensor spacing s helps to remove the ambiguity in damage localization.

In the test case subsection it was proven that the proposed damage localization algorithm allows to localize multiple damage in an isotropic structural element using proposed sensor array. It should be emphasized that the damage localization algorithm does not need baseline data in order to visualize DI. It means that an SHM system based on this idea can be used on a structure without the need for reference (undamaged or previous) measurements. The conducted research showed that directivity of the damage map is strictly correlated with transducer spacing. Better directivity will

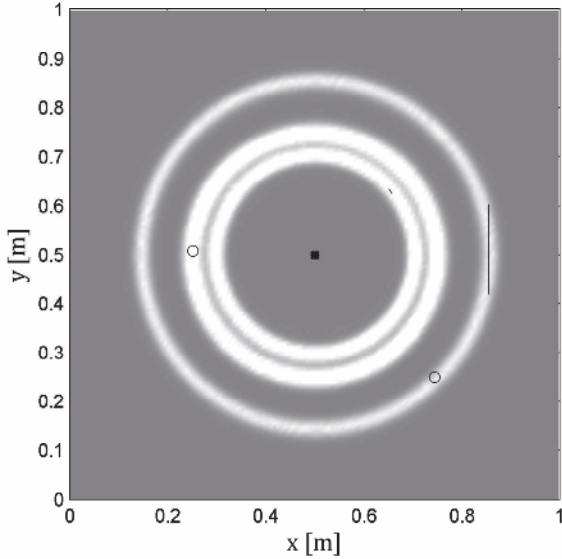


Figure 33. Four defects localization using a square sensor arrays. Circles indicate two holes. Lines indicate notches on specimen surfaces.

be obtained for larger transducer spacings. It was shown that by changing the distance between transducers it is possible to control the damage map directivity. It should also be mentioned that a larger distance between transducers is connected with the fact that a larger portion of the signal is interrupted by wave reflections that occur between transducers. As a result part of the signal connected with reflections between transducers must be rejected and, in effect, a certain area around the transducers cannot be monitored. The presented research showed that it is possible to differentiate the damage states of the structure. The results for one and four defects differ significantly. It means that the proposed DI is a very useful tool.

7 Beam forming algorithm

7.1 Basis for numerical algorithm

In this approach it is also assumed that any discontinuity on the elastic wave propagation path causes wave reflection. In the general approach the sensing configuration consists of N transducers that excite and sense elastic

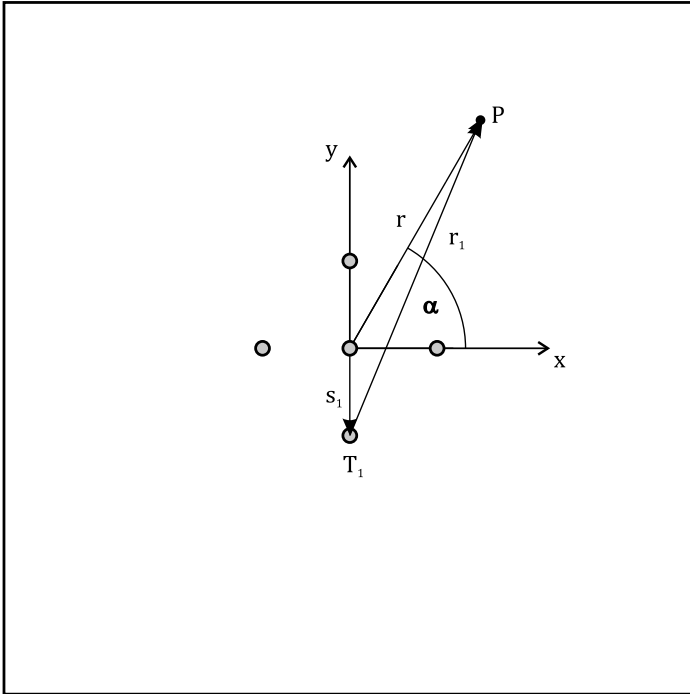


Figure 34. Sensor configuration with illustration of the symbol for beam forming algorithm.

waves. In order to monitor a surface with these transducers they are placed in special manner in points $T_i (i = 1, \dots, N)$. The crucial point in applying this algorithm is that it makes use of the wave interference phenomenon. Assuming a harmonic wave at point \vec{r} at instance t propagating with velocity c one obtain (Giurgiutiu, 2008):

$$f(\vec{r}, t) = \frac{A}{\sqrt{|\vec{r}|}} e^{j(2\pi ft - \vec{k} \cdot \vec{r})}, \tag{21}$$

where A - real amplitude, f - frequency, \vec{k} - wave vector. Using a defined time delays:

$$\Delta(\alpha) = \frac{1 - \hat{r}}{c/|\vec{r}|} \quad (22)$$

$$\Delta(\alpha) = |\vec{r}|/c - |\vec{r}_i|/c \quad (23)$$

$$\Delta(\alpha) = t - t_i, \quad (24)$$

and defined weights for signals registered by T_i sensors:

$$w_i = \sqrt{r_1} \quad (25)$$

a constructive interference for angle α is obtained (Figure 34). The symbol definition is following

$$\hat{r}_1 = \frac{|\vec{r}_m|}{|\vec{r}|}, \quad (26)$$

$$\vec{r}_i = \vec{r} - \vec{s}_i, \quad (27)$$

\vec{s}_m is the position of the i -th sensor, t is the time of wave propagation from the origin to point P , while t_i is the time of wave propagation from sensor T_i to point P (Figure 34). In this way a N -times amplification of the sensor array response is obtained (Giurgiutiu, 2008):

$$S(\vec{r}, t) = N \times f. \quad (28)$$

The amplification can be obtained for wave generation and reception. Wave excitation in each transducer with the delay given by formula 24 results in a constructive interference for point P (Figure 35a). From the other hand if point P is a source of wave, the delays defined by formula 24 can be applied to shift the signals registered by the sensors in an array (Figure 35b). This take into account the difference in time of arrival of the wave front at individual sensors. In the case of Structural Health Monitoring the sensors arrays are used both for wave generation and sensing, therefore the delay algorithm is used twice.

What is important it is not necessary to excite wave with the mentioned delays to obtain interference in wave generation. Application of the delays can be realised in a post processing mode. This mean that waves can be excited sequentially in each transducers and registered by the whole array of N transducers. Next the registered signals are processed by the delay algorithm to simulate the interference both in generation and reception.

In the conducted discussion point P was a source of wave, however in real

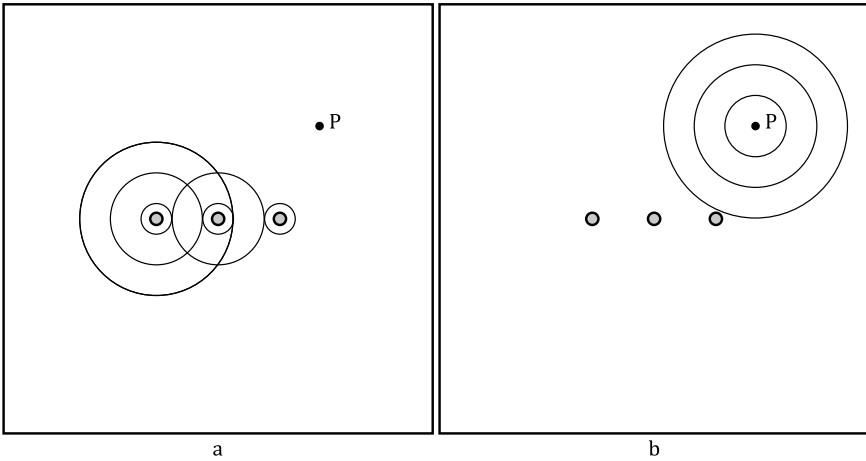


Figure 35. Sensor configuration working in a generation (a) and reception mode (b).

application the source of wave will be damage or other type of discontinuity (rivet, stiffener, etc.). Such discontinuity causes wave reflection, therefore it can be detected. If there is no wave reflection source at chosen point *P* the beam forming algorithm will not give any amplification. This will result in low damage index defined, as before, in the form of squared signal (20).

Characteristics of sensor arrays (phased arrays) Sensor arrays that utilize such beam forming algorithms are called phased arrays. It is important that in order to take advantage of the interference phenomenon the sensors should be placed with a carefully defined spacing. This spacing should be less or equal half of the wavelegh (Malinowski et al., 2008).

$$s \leq \frac{\lambda}{2} \tag{29}$$

This wavelength is of the considered wave, so in the case of Lamb waves the user should define which mode will be used A_0 , A_1 , S_0 , S_1 or other. The Lamb wave dispersion should be also accountned for. Their wavelegh depends on the frequency, therefore if the excitation is broadband several wavelengths are excited and the phased array is tuned only to one of them. This may make damage localization more difficut and dispersion compensation algorithms could be helpful.

The spacing s (29) together with number of sensors N have also an influence

on the precision of sending or receiving of the wave from a certain angle α . In the simplest case - a linear phased array, the dependence is given by the formula (Orfanidis, 2004):

$$W = 0.886 \frac{\lambda}{Ns}. \quad (30)$$

W is the width of the main lobe steered at α angle. If it is narrow, arrays sends waves and is sensitive to the response only from this angle. As an example a directional characteristics of a 3×3 array was calculated. It was plotted in Figure 36. This array was steered at $\alpha = 60^\circ$ and the characteristic was normalised so its maximal value is equal to one. If the condition given by (29) is fulfilled the characteristics of the array unambiguous as in Figure 36a. Waves that are sent and received are related to angles indicated by the main lobe. In the provided example the main lobe is rather wide and in the case of discontinuities lying close to each other, wave reflection from them cannot be differentiated. Following the rule given by (30) an increase in the spacing results in a narrower main lobe. Provided example confirms this. Spacing equal to $s = 2\lambda$ (Figure 36b) ensures a very fine main lobe for $\alpha = 60^\circ$. However this was obtained by the cost of losing the unambiguous characteristic of the array. By choosing spacing $s = 2\lambda$ the condition given by (29) was broken. As an effect one can notice six additional lobes. This phenomena did not facilitate the damage localization and should be avoided. If damage is present at an angle corresponding to any of the additional lobes the information about this will be obtained in the response for the angle $\alpha = 60^\circ$. This will result in false-positive indication of damage for this direction. Using an array with an ambiguous characteristics (as for example this in Figure 36b) should be avoided.

7.2 Results

In this section concerning the beam forming algorithm the experimental example is the same as in the section 6, that concerned energy summing algorithm. Aluminium panel with dimensions of $1000 \text{ mm} \times 1000 \text{ mm} \times 1 \text{ mm}$ was considered as it is presented in Figure 26. Piezoelectric excited waves were registered by the laser vibrometer. Square sensor array was considered as presented in Figure 26a. Piezoelectric transducer with diameter of 10 mm and 0.5 mm thickness was used for excitation of the elastic waves. It was attached at the centre of the panel surface. Excitation signal was in the form of tone burst with frequency 16.5 kHz and 5 periods. As previously the same circular grid of points was chosen for result visualisation.

The first localisation example was obtained for an array of spacing $s = 3$

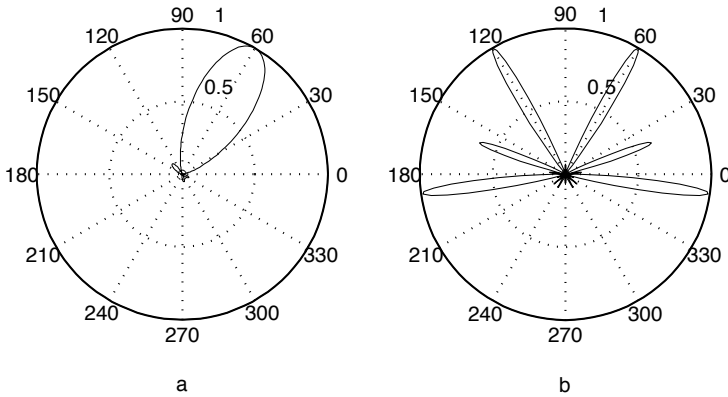


Figure 36. Phased array characteristic dependence on sensor spacing s ; $s = 0.4\lambda$ (a), $s = 2\lambda$ (b)

mm (Figure 37). This result can be directly compared to the example illustrated in Figure 27 for the energy summing algorithm, because parameters (s and N) were identical to the case presented there. As one can notice, thanks to directional properties of the beam forming algorithm the damage localisation is more precise. Damage index value was amplified on the right from the array - in the region of simulated defect. Previous result (Figure 27) indicated only the distance from the array on which the discontinuity was placed. The result presented in Figure 37 can be rather comparable to the result of a 5 array with spacing $s = 30$ mm for which the directivity of the response is more apparent. Increasing the spacing by factor two $s = 6$ mm, results in narrower response for the angle corresponding to discontinuity (Figure 38). However unwanted additional increase of DI appears symmetrical on the left hand side of the array. This is related with the increase in spacing. The case is similar to that presented in Figure 36. The increase of spacing reduced the width of main lobe but this also caused the amplification of the response from other angles. In order to avoid this

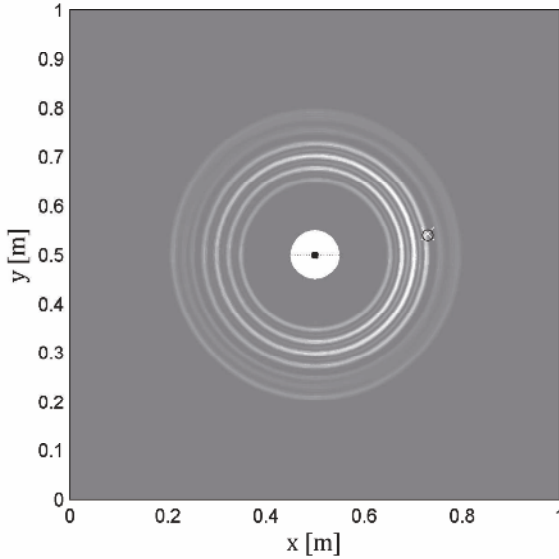


Figure 37. Localization result for a square 3×3 phased array with spacing $s = 3$ mm.

phenomena the spacing should be kept constant and the increase of sensors will help to reduce the main lobe width. This rule is given by formula 30. The next example followed this rule. An array comprising of 25 sensors was selected with smaller spacing $s = 3$ mm. The result was presented in Figure 39. Unambiguous and precise localization was achieved in this way. Although the parameters (s and N) were the same as for energy summing algorithm result presented in 29, this beam forming result is far more accurate.

Test case - CFRP panel The usefulness of the beam forming algorithm was shown on the basis of vibrometer measurement. In this subsection a CFRP panel with permanently attached piezoelectric transducers was investigated. This panel came from a AW139 helicopter and is stiffened by horizontal and diagonal stiffeners indicated in Figures 40 and 41. In order to perform health monitoring five transducers were placed in the middle of the panel forming a cross shaped array. The transducer separation was 2 mm. Rectangular multilayer piezoelectrics were used ($3 \times 3 \times 2$ mm³). After

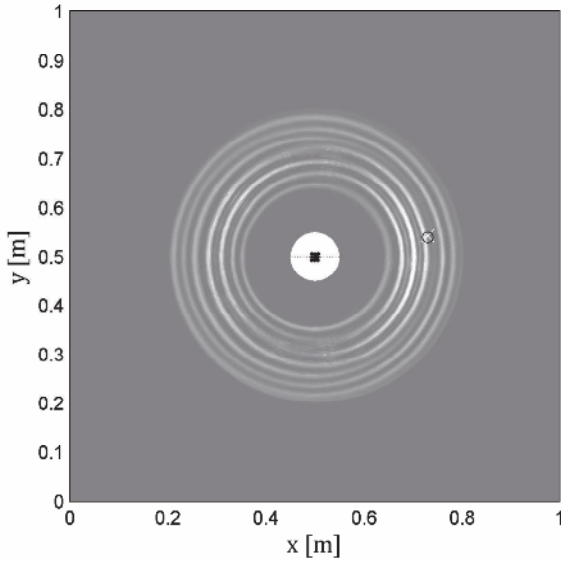


Figure 38. Localization result for a square 3×3 phased array with spacing $s = 6$ mm.

the measurement for pristine plate damage was introduced by hollow metal block impact that was hit by a hammer. Obtained delaminated region was approx. 350 mm^2 . Next the measurements were performed for the damaged panel and a beam forming algorithm was applied. The result for 140 kHz excitation is presented in Figure 40. The measurements were also conducted for other frequencies (100,110,120,130 and 150 kHz) but the localization was less accurate. The maximum of damage index value (indicated by X in Figure 40) differed from the assumed centre of delamination by 43 mm. The next step was the modification of the transducer array. Four more transducers were added to obtain a square array just like this in Figure 26a. In this case the damage index maximum was 45 mm away from the assumed centre of delamination Figure 41. It should be highlighted that in this case 120 kHz excitation gave better result than 140 kHz.

In comparison to cross-shaped array the indication is less accurate. However it is important to underline that in the case of the cross-shaped array baseline information was utilized and the signals were subtracted (damaged state - pristine state). In the subsequent case (square-shaped array) the

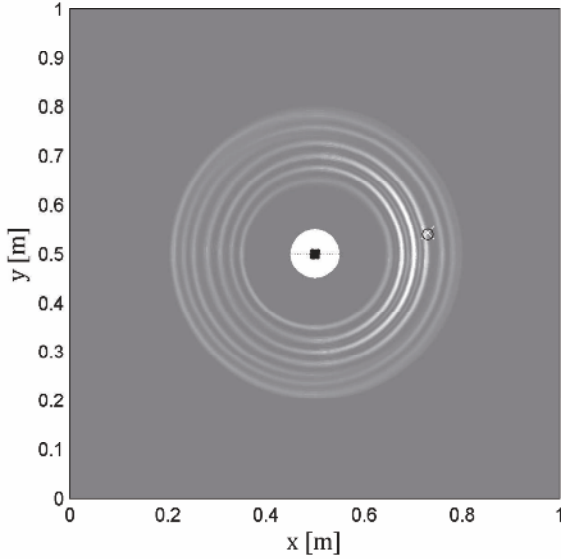


Figure 39. Localization result for a square 5×5 phased array with spacing $s = 3$ mm.

panel was already damaged, so the baseline information was not available.

It should be underlined that measurement on the composite panel was made using only piezoelectric transducers. This approach resulted in more signals for signal processing algorithm because each transducer was sequentially used for wave excitation and the remaining ones for sensing. Due to this measurement scheme for cross-shaped array 20 (5 excitations \times 4 sensors) signals were obtained. In the case of square-shaped array 72 (9 excitations \times 8 sensors) signals were available. If the vibrometry measurement had been concerned, it would have resulted in 5 (1 excitation \times 5 sensing points) signals in the first and 9 in the second case.

The use of an array of transducers influences also the DI visualization (Figure 40 and 41). The DI values for an area around the array were not plotted due to numerous reflection of waves from the sensors. In the case of laser measurement the registered signals at the beginning contain direct waves propagating from the transducer to the sensing points. If the whole transducer array is considered, the signals will not only contain direct waves but also those reflected from the transducers. This initial part of the signals

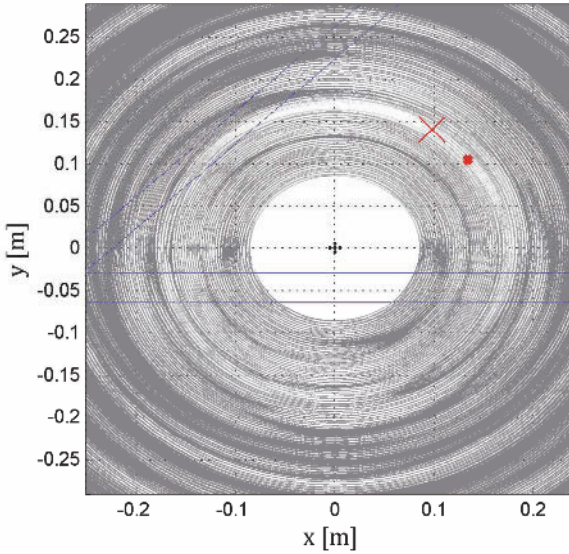


Figure 40. Damage localization result for a CFRP panel with an impact damage. Localization using square-shaped phased array.

was rejected in order not to disturb the visualization of the DI. One can notice that the results obtained for composite panel (Figure 40 and 41) are not so clear and pure as those obtained for vibrometer measurements (Figures 37-39). One reason is that the laser vibrometry measurements for measuring the out-of-plane vibrations so the influence of S_0 mode was negligible, while the piezoelectric transducers register both modes. The second reason is that the signal-to-noise ratio for aluminium panel was higher due to lower attenuation of Lamb waves in aluminium in comparison to CFRP.

7.3 Summary

The beam forming algorithm is a very useful tool in the Structural Health monitoring techniques, that are based on propagation of guided elastic waves. It was shown, that successful application of the algorithm is only possible when a proper transducer spacing s will be chosen. The influence of the spacing and the number of sensor is significant and should be carefully controlled. High precision of damage detection can be obtained, providing the main lobe width is sufficiently narrow. The spacing of a phased array is

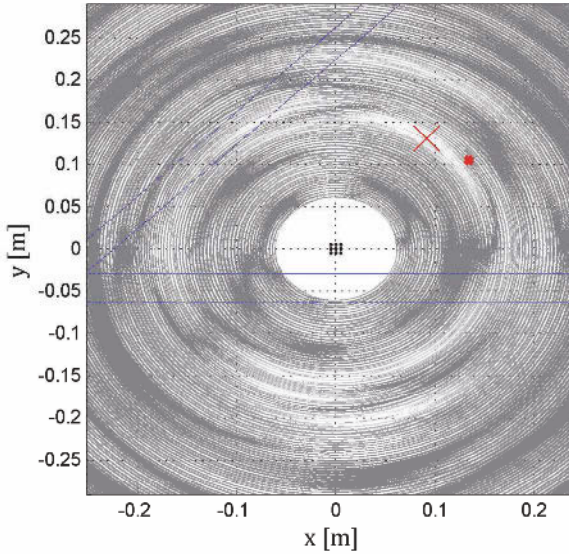


Figure 41. Damage localization result for a CFRP panel with an impact damage. Localization using star-shaped phased array.

chosen in relation to the wavelength (see formula 29). This means that the array should be tuned to previously chosen wavelength of either symmetric or anti-symmetric Lamb wave mode. According to the theory, for the same frequency, A_0 mode wavelength is shorter than S_0 wavelength. This should be taken into account. In the investigation conducted in this section the arrays were tuned for the A_0 mode, because in the laser vibrometry measurements only the out-of-plane signals were taken for signal processing. Regarding the investigation related to aluminium panel it should be emphasized that the damage localization algorithm does not need baseline data in order to visualize DI. It means that an SHM system based on this idea can be used on a structure without the need for reference (undamaged or previous) measurements.

As far as composite panel is concerned, the investigation showed that using only 5 transducers 43 mm accuracy was achieved with baseline data. It was also shown that if there is no information about the healthy structure nine transducers are enough to indicate a defect with a 45 mm accuracy. Presented work proved that phased arrays that were used previously for

aluminium specimen may be successfully utilized for composite structures monitoring.

Obtained results showed high sensitivity of the method. It detected delaminated area of 0.12 % of the monitored area. For instance using vibration methods for delaminated beams only 5 % delaminations were detected (Zak, 2005). In work (Brunner et al., 2008) detection also of 5 % using two other methods: electrical impedance and ultrasonics.

In this chapter authors considered single phased arrays used for SHM. However it is also possible to use a combined approach, that employs few phased arrays working together and giving a cumulative damage index. In a research paper (Malinowski et al., 2011) authors investigated three phased arrays placed in vertices of an equilateral triangle. Each vertex contained a 2×2 array. It was shown that such configuration successfully localizes discontinuities outside and inside of the triangle placed on a aluminium panel surface. Damage detection on the triangle edge was also possible.

Bibliography

- J.-M. Berthelot, M.B. Souda, and Robert. J.L. Frequency response transducers used in acoustic emission testing of concrete. *NDT&E International*, 25(6):279–285, 1992.
- A. J. Brunner, M. Barbezat, N. A. Chrysochoidis, A. K. Barouni, and D. A. Saravanos. Delamination detection in composites using active piezoceramic wafer and AFC sensor. In *Proceedings of 4th European Workshop Structural Health Monitoring (Krakow, Poland, 2-4 July 2008)*, pages 657–664, 2008.
- F. Cau, A. Fanni, A. Montisci, P. Testoni, and M. Usai. A signal-processing tool for non-destructive testing of inaccessible pipes. *Engineering Applications of Artificial Intelligence*, 19:753–760, 2006.
- Y. Ding, R.L. Reuben, and J.A. Steel. A new method for waveform analysis for estimating AE wave arrival times using wavelet decomposition. *NDT&E International*, 37:279–290, 2004.
- S. Dixon and S.B. Palmer. Wideband low frequency generation and detection of Lamb and Rayleigh waves using electromagnetic acoustic transducers (EMATs). *Ultrasonics*, 42:1129–1136, 2004.
- R. Gangadharan, G. Prasanna, M.R. Bhat, C.R.L. Murthy, and S. Gopalakrishnan. Acoustic emission source location and damage detection in a metallic structure using a graph-theory-based geodesic approach. *Smart Materials and Structures*, 18(11), 2009.
- V. Giurgiutiu. *Structural Health Monitoring with piezoelectric wafer active sensors*. Academic Press, Elsevier Inc, 2008.

- V. Giurgiutiu, L. Yu, J.R. Kendall, and C. Jenkins. In situ imaging of crack growth with piezoelectric-wafer active sensors. *AIAA Journal*, 45(11): 2758–2769, 2007.
- K. Hongjoon, J. Kyungyoung, S. Minjea, and K. Jaeyeol. A noncontact NDE method using a laser-generated focused-Lamb wave with enhanced defect detection ability and spatial resolution. *NDT&E International*, 39:312–319, 2006a.
- K. Hongjoon, J. Kyungyoung, S. Minjea, and K. Jaeyeol. Application of the laser-generated focused-Lamb wave for non-contact imaging of defects in plate. *Ultrasonics*, 44:1265–1268, 2006b.
- J.-B. Ihn and F.-K. Chang. Detection and monitoring of hidden fatigue crack growth using a built-in piezoelectric sensor/actuator network: I. diagnostics. *Smart Materials and Structures*, 13:609–620, 2004.
- J.-B. Ihn and F.-K. Chang. Pitch catch active sensing methods in structural health monitoring for aircraft structures. *Structural Health Monitoring, An International Journal*, 7 (1):5–19, 2008.
- H. Jeong. Analysis of plate wave propagation in anisotropic laminates using a wavelet transform. *NDT&E International*, 34:185–190, 2001.
- G.R. Kirikera, J.W. Lee, M.J. Schulz, A. Ghoshal, M.J. Sundaresan, R.J. Allemang, V.N. Shanov, and H. Westheider. Initial evaluation of an active/passive structural neural system for health monitoring of composite materials. *Smart Materials and Structures*, 15:1275–1286, 2006.
- T. Kundu, S. Das, S.A. Martin, and K.V. Jata. Locating point of impact in anisotropic fiber reinforced composite plates. *Ultrasonics*, 48:193–201, 2008.
- R. Lammering. Observation of piezoelectrically induced wave propagation in thin plates by use of speckle interferometry. *Experimental Mechanics*, 50:377–387, 2010.
- C.M. Lee, J.L. Rose, and Y. Cho. A guided wave approach to defect detection under shelling in rail. *NDT&E International*, 42:174–180, 2009.
- Y.S. Lee, D.J. Yoon, S.I. Lee, and J.H. Kwon. An active piezo array sensor for elastic wave detection. *Key Engineering Materials*, 297-300:2004–2009, 2005.
- W. Lestari and P. Qiao. Application of wave propagation analysis for damage identification in composite laminated beams. *Journal of Composite Materials*, 39:1967–1984, 2005.
- M. Lin and F.-K. Chang. The manufacture of composite structures with a built-in network of piezoceramics. *Composites Science and Technology*, 62:919–939, 2002.
- P. Malinowski, T. Wandowski, and W. Ostachowicz. Multi-damage localization with piezoelectric transducers. In *Proceedings of 4th European Workshop on Structural Health Monitoring*, pages 716–723, 2008.

- P. Malinowski, T. Wandowski, and W. Ostachowicz. Damage detection potential of a triangular piezoelectric configuration. *Mechanical Systems and Signal Processing*, 25:2722–2732, 2011.
- M. Melnykowycz, X. Kornmann, C. Huber, M. Barbezat, and A. J. Brunner. Performance of integrated active fiber composites in fiber reinforced epoxy laminates. *Smart Materials and Structures*, 15(1):204–212, 2006.
- M. Melnykowycz, M. Barbezat, R. Koller, and A. J. Brunner. Packaging of active fiber composites for improved sensor performance. *Smart materials and structures*, 19(1):015001, 2010.
- J. E. Michaels, A. J. Croxford, and P. D. Wilcox. Imaging algorithms for locating damage via in situ ultrasonic sensors. In *Proceedings of the 2008 IEEE Sensors Applications Symposium*, pages 63–67, 2008.
- R. Murayama and K. Mizutani. Conventional electromagnetic acoustic transducer development for optimum Lamb wave modes. *Ultrasonics*, 40:491–495, 2002.
- F. Mustapha, G. Manson, K. Worden, and S.G. Pierce. Damage location in an isotropic plate using a vector of novelty indices. *Mechanical Systems and Signal Processing*, 21:1885–1906, 2007.
- S. J. Orfanidis. *Electromagnetic waves and antennas*. <http://www.ece.rutger.edu/orfanidi/ewa>, 2004.
- W. Ostachowicz and P. Kudela. Experimental verification of the Lamb-wave based damage detection algorithm. In *Proceedings of 6th International Workshop on Structural Health Monitoring*, pages 2066–2073, 2007.
- W. Ostachowicz, P. Kudela, P. Malinowski, and T. Wandowski. Damage localisation in plate-like structures based on PZT sensors. *Mechanical Systems and Signal Processing*, 23:1805–1829, 2009.
- M. Palacz, M. Krawczuk, and W. Ostachowicz. The spectral finite element model for analysis of flexural-shear coupled wave propagation. part 1: Laminated multilayer composite beam. *Composite Structures*, 68:37–44, 2005.
- I.-K. Park, T.-H. Kim, H.-M. Kim, Y.-K Kim, Y.-S. Cho, and W.-J. Song. Evaluation of hidden corrosion in a thin plate using a non-contact guided wave technique. *Key Engineering Materials*, 321-323:492–496, 2006.
- P.X Qing, S. Beard, S.B. Shen, S. Banerjee, I. Bradley, M.M. Salama, and F.-K. Chang. Development of a real-time active pipeline integrity detection system. *Smart Material and Structures*, 18:1–10, 2009.
- X.P. Qing, S.J. Beard, A. Kumar, H.-L. Chan, and R. Ikegami. Advances in the development of built-in diagnostic system for filament wound composite structures. *Composites Science and Technology*, 66:1694–1702, 2006.
- J.L. Rose. *Ultrasonic waves in solid media*. Cambridge University Press, 2004.

- D. Royer and E. Dieulesaint. *Elastic waves in solids II. Generation, Acousto-optics interaction, applications*. Springer, 1999.
- A. Rytter. Vibration based inspection of civil engineering structures. Ph.D. Dissertation, Department of Building Technology and Structural Engineering, Aalborg University, Denmark, 1993.
- K.I. Salas and C.E.S. Cesnik. Guided wave excitation by a clover transducer for structural health monitoring: theory and experiments. *Smart Materials and Structures*, 18:1–27, 2009.
- M.H.S. Siqueira, C.E.N. Gatts, R.R. da Silva, and J.M.A. Rebello. The use of ultrasonic guided waves and wavelets analysis in pipe inspection. *Ultrasonics*, 41:785–797, 2004.
- Z. Su, C. Yang, N. Pan, L. Ye, and L.M. Zhou. Assessment of delamination in composite beams using shear horizontal (SH) wave mode. *Composites Science and Technology*, 67:244–251, 2007.
- N. Takeda, Y. Okabe, J. Kuwahara, S. Kojima, and Ogisu. T. Development of smart composite structures with small-diameter fiber Bragg grating sensors for damage detection: Quantitative evaluation of delamination length in CFRP laminates using Lamb wave sensing. *Composites Science and Technology*, 65:2575–2587, 2005.
- A.B. Thien, editor. *Pipeline structural health monitoring using macro-fiber composite active sensors*, 2006. Ph.D. Dissertation, College of Engineering, University of Cincinnati.
- G. Thursby, B. Sorazu, D. Betz, W. Staszewski, and B. Culshaw. Comparison of point and integrated fiber optic sensing techniques for ultrasound detection and location of damage. In *Proceedings of SPIE*, volume 5384, pages 287–295, 2004.
- C. Valle and J.W. Jr. Littles. Flaw localization using the reassigned spectrogram on laser-generated and detected Lamb modes. *Ultrasonics*, 39: 535–542, 2002.
- D. Wagg, I. Bond, P. Weaver, and M. Friswell. *Adaptive Structures. Engineering Applications*. John Wiley & Sons Ltd, 2007.
- P.D. Wilcox, editor. *Lamb wave inspection of large structures using permanently attached transducers*, 1998. Ph.D. Dissertation, Imperial College of Sciences, London.
- K. Worden and J.M. Dulieu-Barton. An overview of intelligent fault detection in systems and structures. *Structural Health Monitoring, An International Journal*, 3(1):85–98, 2004.
- L. Yu, G. Santoni-Bottai, B. Xu, W. Liu, and V. Giurgiutiu. Piezoelectric wafer active sensors for in situ ultrasonic-guided wave SHM. *Fatigue & Fracture of Engineering Materials & Structures*, 31:611–628, 2008.
- A. Zak. Non-linear vibrations of a delaminated composite beam. *Key Engineering Materials*, 293-294:607–616, 2005.

G. Zumpano and M. Meo. A new damage detection technique based on wave propagation for rails. *International Journal of Solids and Structures*, 43: 1023–1046, 2006.